Comparative FE Study between MAT159 and MAT072R3 for Concrete Behaviour Modelling under Quasi-static Loading in LS-DYNA

by

Tan Jor Yi

16552

Dissertation submitted in partial fulfilment of
the requirements for the
Bachelor of Engineering (Hons)
(Civil)

JANUARY 2016

Universiti Teknologi PETRONAS
32610 Bandar Seri Iskandar
Perak Darul Ridzuan
Malaysia

CERTIFICATION OF APPROVAL

Comparative FE Study between MAT159 and MAT072R3
for Concrete Behaviour Modelling under Quasi-static Loading in LS-DYNA

by

Tan Jor Yi

16552

A project dissertation submitted to the

Civil Engineering Programme

Universiti Teknologi PETRONAS

in partial fulfilment of the requirement for the

BACHELOR OF ENGINEERING (Hons)

(CIVIL)

Approved by,

_____

(DR. TEO WEE)

UNIVERSITI TEKNOLOGI PETRONAS

TRONOH, PERAK

January 2016

CERTIFICATION OF ORIGINALITY

This is to certify that I am responsible for the work submitted in this project, that the original work is my own except as specified in the references and acknowledgements, and that the original work contained herein have not been undertaken or done by unspecified sources or persons.

Joryi

TAN JOR YI

ABSTRACT

FE programs have been widely used to study behaviour of reinforced concrete, owing to the complexity and nonlinearity of reinforced concrete which cause analytical methods to be impractical. LS-DYNA has gained its position for conducting quasi-static simulation using transient dynamic analysis in the recent years. Material models MAT159 and MAT072R3 are used extensively in concrete behaviour modelling as they require the least input from user, among all other concrete material models. Therefore, the behaviour and reliability of both material models, which are formed on the basis of varying failure surfaces, used for simulating reinforced concrete beams under quasi-static loading are of interest. A comparative study between MAT159 and MAT72R3 is carried out to investigate the flexural and shear behaviour of reinforced concrete beams loaded under quasi-static loading, which is a displacement-controlled static loading, using selected specimens of control beam tested experimentally by various researchers. FE results such as load-deflection curves and failure modes are compared to those of the experimental works to verify the behaviour and reliability of the material models being tested. Results shown that MAT159 is more reliable than MAT072R3 in terms of modelling flexural behaviour of reinforced concrete beam under quasi-static loading. In the case of shear behaviour, both material models do not show reliable response hence require further simulation tests to be carried out.

ACKNOWLEDGEMENT

First and foremost, I would like to express my gratitude to people who have helped, encouraged, and supported me during this period of Final Year Project. Throughout these few months of FYP works, I have received a lot of guidance and assistance in completing the research. I truly appreciate these and strongly believe that I have gained valuable skills and knowledge that would be useful for my future path of career.

Special thanks to my supervisor, Dr. Teo Wee, who have guided me and taught me knowledge and skills in the midst of completing this research for FYP. He has been willingly and generously sharing his knowledge and experience so that I can learn from it. It has been a pleasure to work with him in this research and I have gained much from witnessing how he resolves issues arose in this project.

Last but not least, a very big thank you to my family for their unconditional care and support. They have given me remarkable source of energy and willpower that keeps me motivated in doing my best throughout the whole period of FYP.

Table of Contents

List of Figures

List of Tables

CHAPTER 1

INTRODUCTION

1.0 Background

Finite element method (FEM) is one of the most crucial methods of numerical simulation used in recent decades for modelling of various physical phenomena. With mathematical models, namely sets of equations associated with the law of physics, FEM is complemented and made useful for researchers, engineers, and scientists to predict or approximate the behaviour of the subject of interest, nevertheless, with minimal errors. It involves individually or a combination of algebraic, differential, and/or integral equations to form a relationship between parameters associated with the engineering problem to be solved, precisely (Reddy, 1993).

In structural engineering point of view, FEM is widely used for modelling of reinforced concrete (RC) damage behaviour. It is essentially a method of breaking down a structural component, e.g. a reinforced concrete beam, into discrete and relatively small parts, known as elements, subsequently determining the governing equation for this engineering problem and hence formulating the relevant equations fit to each of the discrete elements, and eventually clustering all elements in terms of these equations and their inter-element relationships to put all elements back into the original form of the structural component, consequently simulating the actual behaviour of the structural component by using a system of equations. The end results would be the anticipated solution incorporated with appropriate functions to minimize erroneous approximations (Reddy, 1993).

Why FEM is of utmost importance in the present era in structural engineering? Why researchers and engineers study and use FEM to solve structural problems? An attempt of using analytical models to solve complex problems was done initially.

However, as development took place and created sophisticated materials, shapes, geometries, structural loads, and nonlinearities of structural components, analytical models become less capable of expressing the complexities of the engineering problem (NPTEL, 2014; Reddy, 1993). Plus, some properties and behaviours of RC that are significant in the sense of structural performance, which are non-homogenous and nonlinear, make analytical models extremely complicated and impractical, aside from the monolithic nature of RC structures, composite action between concrete body and steel reinforcements, as well as inherent variability of concrete (Rajagopal, 1976; Suidan & Schnobrich, 1973). This is how FEM comes into picture to enable researchers and engineers to solve complex structural problems, with effective use of current technological advancement.

Since the 1970s, FEM has been used extensively to study damage behaviours of RC components, which include stress and strain response, deflection, cracking, as well as failure mode of the RC elements (Suidan & Schnobrich, 1973). It enables researchers to perform parametric studies on relevant factors affecting behaviours of RC components. Rather than conducting tedious and time-consuming experimental works, FEM provides an alternative for researchers or engineers to better understand a material, provided that validation works are done for FEM models in prior. On top of that, with good engineering knowledge and understanding of the theory adopted in FEM, relevant input parameters can be defined so as to better simulate the actual behaviour of RC components. Computer also made FEM more feasible as it allows quicker and automated computational works. With regards to the computational time, it depends largely on the size of elements being modelled, relative to the overall size of the components of interest (Reddy, 1993).

The evolution of FEM is apparent with advancement in technology over the last 50 years. One of the earliest applications of FEM in RC structures was in 1967, started off with a linear elastic analysis characterized with pre-defined cracks and bond-slip behaviour between concrete body and steel reinforcements. Gradually, non-linear properties and relationships which are relevant to a RC structure are introduced into FEM, apart from extension to the entire range of loading. Subsequently, factors of

creep and shrinkage, influence of temperature, and inelastic analysis are incorporated as well. Further to that, one of the researchers has also developed an expression defining crack width in terms of strain. Next, non-linear bending behaviour of RC components was successfully modelled, thus leading to development of an approach to predict time-dependent deflections of RC members. And then, in-plane and out of plane (bending) stiffness of RC structures are also simplified and then assumed appropriately within the FEM simulations. Curved surfaces had also taken place at that time in FEM, modelled by using flat triangular elements. FEM works had also been extended to investigation of RC behaviour under biaxial stresses (Rajagopal, 1976). These are the advancements of FEM for reinforced concrete in the field of structural engineering that can be seen in the 1960s and 1970s, which have tremendously contributed to the innovation of FEM in subsequent decades until today.

In the past decade, FEM has remained an everlasting impression in the industry, in conjunction with the development of supercomputers as well as abundant computer software for structural analysis by using FEM. More complex problems can be solved more easily and within a shorter duration with these finite element programs. Some of the most commonly used FE programs for researchers are ABAQUS, ANSYS, and LS-DYNA (Cotsovos et al., 2009). In this research, LS-DYNA is used for the FE study.

LS-DYNA is a general purpose FE program which enables simulation of real world complex engineering problems, developed by Livermore Software Technology Corporation (LSTC). Generally, LS-DYNA is designed for transient dynamic analysis of highly nonlinear problems, in which explicit time integration method is used in generating solution properties. By transient analysis, it means that the problem involves highly dynamic excitation occurred in a relatively short duration, which makes the inertial and damping effects significant enough to be taken into account for structural analysis, for instance. By explicit, it means that central difference method is used in the FE program as its direct integration method. Explicit numerical analysis involves computation of dependent variables in terms of known

quantities, on the basis of the equation of motion ($F = m\ddot{x} + c\dot{x} + kx$). In relative to an implicit solution, explicit integration method saves computational time, without having to perform neither iterative techniques nor convergence control as in the case of implicit integration method (Linde et al., 2006; Liu, 2008; LSTC, 2011; Rust & Schweizerhof, 2003).

Quasi-static simulation is one of the main applications of LS-DYNA. The reason it is called a quasi-static simulation is because of the mechanism used to solve quasi-static problem, which is as mentioned, an explicit dynamic analysis. In quasi-static simulation, the ultimate aim is to carry out the analysis while making sure that the inertial and damping effect of the subject are well below the limit and thus become negligible. With this condition being fulfilled, the equation of static analysis ($F = kx$) is satisfied, thus generating results which have simulated the actual properties or behaviour of the subject, say, a reinforced concrete beam in this context as close as possible (LSTC, 2003; Rust & Schweizerhof, 2003).

To model the subject of interest in LS-DYNA, the nonlinear FE program provides a wide library of material properties including for metals, plastics, glass, foams, fabrics, viscous fluids, and concrete (LSTC, 2011). For concrete material, there are four most commonly used concrete material properties as provide in LS-DYNA's library. These include:

- Mat Concrete Damage Release III (MAT072R3),
- Mat Winfrith (MAT084),
- Mat Continuous Surface Cap Model (CSCM) Concrete (MAT159), and
- Mat Riedel, Hiermaier and Thoma (RHT) Model (MAT272) (Hallquist, 2007; Magalhaes Pereira et al., 2013; Wu et al., 2014).

However, in this research, MAT072R3 and MAT159 remain as the focus as several researches have proven that two of these material models are capable of predict and

represent the actual concrete behaviour, either under dynamic loading or quasi-static loading.

1.1 Problem Statement

LS-DYNA has been widely used in numerous researches to simulate and study reinforced concrete behaviour under various kind of condition. As LS-DYNA is a transient-dynamic-analysis-based FE program, it has been used extensively for dynamic analysis associated with blast loading or impact loading. Some of the RC structural components being researched include beams, columns, slabs, concrete frames (system of beams, columns, and slabs), beam-column connections, composite sections, steel beams, bridge piers, railway sleepers, etc. Several dynamic analyses related to progressive collapse have also been carried out by using LS-DYNA. This has shown the versatility the FE program offers, which has gained attention in FE branch of structural engineering.

Despite its popularity among dynamic analyses, LS-DYNA is also capable of simulating quasi-static condition associated with RC structures. It is a challenge to ensure that the inertial forces and damping forces are substantially low enough to not affect the static system. A number of researchers have carried out quasi-static simulation using LS-DYNA to study behaviours of RC structural components under quasi-static loading condition and they have shown promising FE results, but it still remains under-researched. By under-researched, it means that limited researches have been done on quasi-static simulation by using LS-DYNA to study flexural and shear behaviour of RC beams, for instance.

Previous studies have shown that quasi-static simulation by using LS-DYNA is compatible with experimental test for researches studying flexural and shear behaviour of RC beams. However, limited database for quasi-static simulation among the literature, particularly for shear behaviour of RC beams, makes such study more important and in need to be further investigated by using LS-DYNA.

Apart from that, current available literature has only provided a vague account on quasi-static simulation on behaviours of RC beams. While quasi-static simulation on RC beams behaviour using MAT159 and MAT072R3 has just been limitedly investigated and there is no such researches performing direct comparison between the two material models, simultaneously this research would be extended to using both material models available in the LS-DYNA material library.

1.2 Objectives and Scope of Study

The objectives of the research "Comparative FE Study between MAT159 and MAT072R3 for Concrete Behaviour Modelling under Quasi-static Loading in LS-DYNA" are as follow:

- To compare MAT159 and MAT072R3, by simulating flexural and shear behaviours of RC beams, in terms of failure mode and load-deflection curves using LS-DYNA.
- To study relevant input parameters of MAT159 and MAT072R3 and their effects on behaviour of concrete or RC beam, in terms of stress-strain relationship curves or load-deflection curves.

In particular, this research would involve extensive use of non-linear finite element modelling to study the RC behaviour and to validate selected RC beams. Rectangular RC beams are of interest in this research, tested under three-point bending or four-point bending, involving displacement-controlled quasi-static loading. Strain rate effects will not be taken into consideration. At the end of the research, several output parameters will be determined:

i. Load
ii. Mid-span deflection of the beam
iii. Relationship between load and mid-span deflection
iv. Failure mode of the beams
v. Comparison between experimental results and FEM results

CHAPTER 2

LITERATURE REVIEW

2.0 Introduction

This section of the report comprises analysis of past researches with regards to quasi-static simulation on behaviour of RC beams by using LS-DYNA, as well as review of the FE program itself.

2.1 Review of Existing Literature

A review of existing literature has been done on RC beam behaviour modelling using LS-DYNA, as shown in Table 2.1 as follows. As mentioned in Section 1.1, LS-DYNA has been extensively used for dynamic analysis to study behaviour of RC beams under impact or blast loading, and this is shown clearly in Table 2.1.

Compared to behavioural study of RC beams under quasi-static loading, researchers were more interested to employ LS-DYNA in investigation of structural response under impact or blast loading, as that is what LS-DYNA is designed for. Some of the issues being addressed associated with blast loadings include:

- progressive collapse of buildings (Yi et al., 2007; X. H. Zhang et al., 2011),
- protective structures against impact load, e.g. nuclear power plants, fuel tanks, etc. (Bhatti et al., 2009),
- threat and terrorisms involving bombing and explosion (Li & Hao, 2011; Mohammed & Parvin, 2011; Yoon et al., 2013),
- and natural disasters such as earthquakes, falling rocks and avalanche (Adhikary et al., 2012; Kishi et al., 2011; Yoon et al., 2013).

Behaviour or properties of RC beams under blast / impact loading in which researchers are concerned about and interested to investigate include:

Table 2.1: Compilation of Existing Literature on Behaviour of RC Beam Study Using LS-DYNA

				Section Geometry		Loading			Failure Mode Studied		Concrete MAT			
No	**Research Topic**	**Author**	**Year**	**Rectangular**	**Square**	**Static / Quasi-static**	**Blast/ Impact**	**Varying Rates**	**Flexural**	**Shear**	**MAT159**	**MAT072R3**	**Others**	**Not Mentioned**
1	Finite Element Simulation of Blast Loads on Reinforced Concrete Structures using LS-DYNA	Yi et al.	2007	■			■		■	■			■	
2	Elasto-plastic Impact Response Analysis of Shear-failure-type RC Beams with Shear Rebars	Bhatti et al.	2009	■			■			■				■
3	Finite Element Modelling of Strcutural Concrete	Cotsovos et al.	2009	■		■	■		■	■		■	■	
4	Numerical Simulation for Failure Modes of Reinforced Concrete Beams under Blast Loading	Zhang et al.	2010	■			■		■	■			■	
5	Numerical Simulation of Reinforced Concrete Beams under Consecutive Impact Loading	Kishi et al.	2011	■			■		■					■
6	A Two-step Numerical Method for Efficient Analysis of Structural Response to Blast Load	Li & Hao	2011	■			■		■	■		■		
7	Impact Load Response of Concrete Beams Strengthened with Composites	Mohammed & Parvin	2011	■			■		■		■			
8	Experimental and Numerical Study for the Shear Strengthening of RC Beams Using TRM	Al-Salloum et al.	2012	■		■				■	■			
9	Dynamic Behaviour of Reinforced Concrete Beams under Varying Rates of Concentrated Loading	Adhikary et al.	2012	■				■	■	■		■		
10	Numerical Simulation of Impact Tests on Reinforced Concrete Beams	Jiang et al.	2012	■			■		■	■			■	
11	Strength and Behaviour in Shear of RC Deep Beams under Dynamic Loading Conditions	Adhikary et al.	2013	■				■		■		■		
12	Experimental and Numerical investigation for the Flexural Strengthening of RC Beams Using Near-surface Mounted Steel or GFRP Bars	Almusallam et al.	2013	■		■			■		■			
13	Flexural Strengthening of RC Beams Using TRM - Experimental and Numerical Study	Elsanadedy et al.	2013	■		■			■		■			
14	Improved Impact Resistance of Layered Steel Fiber Reinforced Concrete Beam	Yoon et al.	2013	■			■		■			■		
15	Effect of Longitudinal Steel Ratio on Behaviour of RC Beams Strengthened with FRP Composites	Almusallam et al.	2014	■		■			■		■			
16	Low Velocity Impact Response of RC Beams: Experimental and Numerical Investigation	Adhikary et al.	2015	■			■		■	■	■			
17	Numerical Analysis of Prestressed Reinforced Concrete Beam Subjected to Blast Loading	Chen et al.	2015	■			■		■	■		■		
18	Structural Evaluation of RC Beams Strengthened with Innovative Bolted/Bonded Advanced FRP Composites Sandwich Panels	Mosallam et al.	2015		■	■			■		■			

- Effects of load generation, time step, and mesh size on simulation results (Yi et al., 2007),
- Development of design approach on performance-based impact resistance (Kishi et al., 2011),

- Better FE approach to reduce the computational time yet maintaining or improve the reliability of results (Li & Hao, 2011),
- Effects of consecutive impact loading on accumulated damage and residual load-carrying capacity of RC beams (Kishi et al., 2011),
- Effect of loading rates on flexural and shear structural behaviour of RC beams (Adhikary et al., 2012, 2013, 2015), etc.

From the dynamic analysis of RC beams under impact / blast loading, some researchers have found that LS-DYNA could produce rather similar results as compared to experimental results, thus proven the reliability of the material models available in LS-DYNA library. As shown in Table 2.1, MAT072R3 is more widely accepted for dynamic analysis of RC beams under impact loadings, as compared to MAT159. Only Cotsovos et al. (2009) have studied flexural and shear behaviour of RC beams under quasi-static loading using MAT072R3, and have shown close correlation to experimental results. However, with limited database available in the existing literature, it is questionable such that whether MAT072R3 is capable of simulating the actual behaviour of RC beams.

On the other hand, for static or quasi-static simulation using LS-DYNA, MAT159 is more generally accepted by researchers, such as Al-Salloum (2012), Almusallam et al. (2013), Elsanadedy et al. (2013), Almusallam et al. (2014), and Mosallam et al. (2015), and have shown FE results that are excellently agreed to the experimental results, in respective journals. However, most have only studied the flexural behaviour of RC beams under quasi-static loading using MAT159 in LS-DYNA, while only Al-Salloum (2012) have studied shear behaviour of RC beams modelled with MAT159 subjected to quasi-static loading.

Consequently, in this research, FE simulations are to be extended to comparatively study flexural as well as shear behaviour of RC beams subjected to quasi-static loading specifically, so as to have a better idea about the behaviour of both material models.

2.2 Quasi-static Simulation

As mentioned in previous section, LS-DYNA is designed for general transient analysis, which means the algorithms lies within the simulation take inertia forces and damping forces into consideration when solution is being computed. In the case of a quasi-static simulation, however, both of these forces are to be eliminated or kept low to a negligible extent (Linde et al., 2006; Rust & Schweizerhof, 2003).

Noted that the load application in LS-DYNA is time-history dependent, quasi-static simulation can be explicitly modelled such that the static loading test is performed using displacement-controlled static loading, which can be defined in keyword PRESCRIBED_MOTION. A constant velocity is to be assigned for load application so as to avoid any inertia forces or acceleration that could yield results as in the case of dynamic or impact loading test. The velocity defined depends on the researchers, either to match with actual experimental loading or to be judged with good engineering knowledge (Almusallam et al., 2015).

As studies have suggested that loading rate has an effect on the strength of the concrete, the constant velocity defined in keyword DEFINE_CURVE should be done with reasonable justification (Adhikary et al., 2012, 2013). Too fast of the defined velocity might turn the problem into an impact simulation. To ensure the transient analysis remains a static or quasi-static condition, the kinetic energy of the RC beam should be considerably low as compared to the internal energy of the system. Another way of the static check is to ensure that the system is in static equilibrium by making sure that transverse force of a given cross section and the fixed end is constant, while the moments should exhibit a linear pattern (Rust & Schweizerhof, 2003).

2.3 MAT Continuous Surface Cap Model (CSCM) - Concrete (MAT159)

Material model MAT159 has given users two options, in which to input own material properties, or to use default material properties for normal strength concrete

ranging from 20 MPa to 58 MPa, with emphasis on mid-range between 28 MPa to 48 MPa. For most cases, MAT_CSCM_CONCRETE under MAT159 is adopted for sake of simplicity and convenience. In case of calibration of material model is in need, MAT_CSCM can be used on the other hand. Material model MAT159 is formed on the basis of a cap model as shown in Figure 2.4, in which a cap model is simulated with smooth intersection between the shear yield surface and hardening cap (Hallquist, 2007; Murray, 2007; Murray et al., 2007).

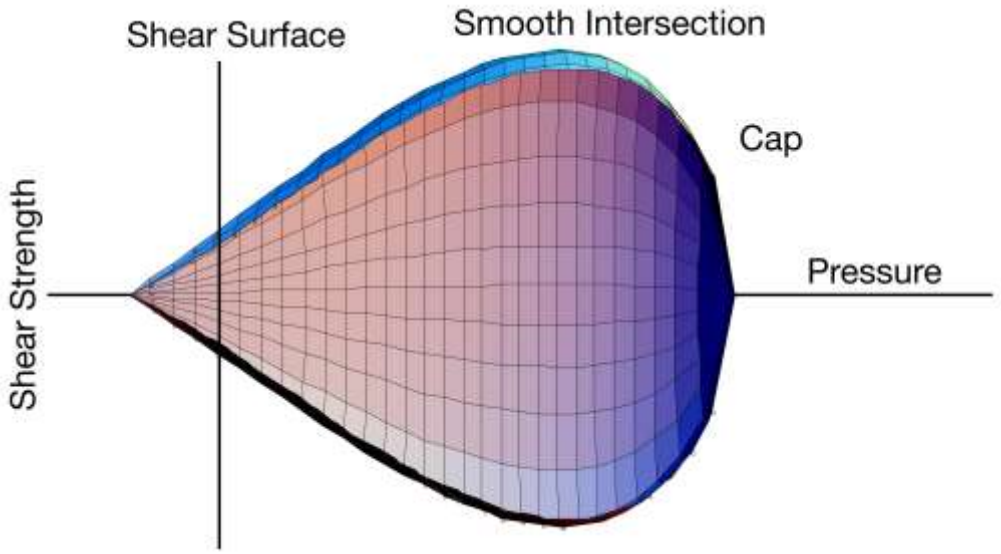

Figure 2.1: Cap model, used in material model MAT159, governing the behaviour of concrete model.

For material model MAT159, MAT_CSCM_CONCRETE, it requires users to input three important parameters, i.e. unconfined compressive strength of concrete, aggregate size, and units the user wish to use. Given that the input of unconfined compressive strength of concrete is within the range as mentioned, it will have an effect on stiffness, three-dimensional yield strength, hardening, and damage-based softening. Only aggregate sizes between 8mm and 32mm are applicable, which in turns have an effect on only the softening behaviour of the damage formulation. In order to exhibit the actual condition of erosion of concrete, wherein cracking and spalling normally occur upon failure, an erosion (ERODE) value is input to simulate such phenomenon. It is recommended that ERODE value can be specified as 1.05 or 1.10 to simulate erosion of concrete elements when they reached a maximum principal strain of 5% to 10% (Mosallam et al., 2015; Murray, 2007; Murray et al., 2007).

2.4 MAT Concrete Damage Release III (MAT072R3)

MAT072R3 is a revision material model of MAT072 that has been used "to analyse buried steel reinforced concrete subjected to impulsive loadings". It is a coupled plasticity-damage model as well as a three-invariant model, employing a multi-yield surface approach using three shear failure surfaces. Yield strength, ultimate strength, and the residual strength of the material model are expressed as a function of damage accumulation in compression and tension (Cotsovos et al., 2009; Hallquist, 2007).

Using this material model requires inputs such as mass density, unconfined compression strength of concrete (as negative value for compression), unit conversion factor for length (RSIZE) and stress (UCF) in case of when SI units are used, as well as load curve in case of strain-rate effects are considered for any particular reinforced concrete structural element (Abraham & Ong, 2015; Hallquist, 2007).

To define the modulus of elasticity of MAT072R3, an Equation of State keyword, EOS_TABULATED_COMPACTION will be auto-generated with the value input of unconfined compressive strength. A set of values are generated in the form of pairs of pressure and corresponding volumetric strain (Cotsovos et al., 2009; Hallquist, 2007; Schwer & Malvar, 2005), which slope of the relationship of the both properties directly represents bulk modulus of the concrete material model. The following relationship shows how modulus of elasticity is related to bulk modulus,

$$Elasticity\ modulus, E = 3K(1 - 2\nu)$$

where K is bulk modulus and ν is Poisson's ratio. If appropriate adjustment of modulus of elasticity is required, the values of second point or pair of pressure versus volumetric strain can be modified according to experimental tests, in order to simulate the actual properties of concrete material. Prior to making modification in the pressure vs volumetric strain card in EOS_TABULATED_COMPACTION, all input parameters in all cards of MAT072R3 shall be input manually in order to generate behavior of concrete according to the defined Equation of State. Values of input parameters for MAT072R3 as well as EOS_TABULATED_COMPACTION

can be found in messag or d3hsp file generated after the first run of simulation with default input of parameters as mentioned in the previous paragraph (Hallquist, 2007; Schwer & Malvar, 2005).

2.5 Miscellaneous Modelling Techniques

In modelling using LS-DYNA, several journals have been referred to as reference or for validation purposes. Some of the important parameters taken into account include model geometry, material modelling for steel reinforcement, boundary conditions, and erosion of element in the finite element model (Almusallam et al., 2015; Elsanadedy et al., 2013; Mosallam et al., 2015).

In model geometry, to model the actual behaviour of the RC beams, the concrete body of the beam is modelled using 8-node reduced integration solid hexahedron elements. Steel rebars including main reinforcement and steel stirrups are modelled as 2-node Hughes-Liu beam elements, while FRP regardless of its nature of system is modelled as 4-node shell elements (Almusallam et al., 2015; Elsanadedy et al., 2013; Mosallam et al., 2015).

With regards to size of solid elements to be modelled, it is dependent on the mesh convergence test. Mesh convergence test is essential in determining the size of mesh to be used for the simulation, as the optimum size of elements would ensure a converged result. This means that a further decrease of element size will only have minimal effect on the overall results. Despite the fact that the smaller element size would lead to a more accurate finite element analysis thus results, as long as the minimal effect is achieved, the optimum element size should be used in order to optimize computational time as well as computer memory required (Elsanadedy et al., 2013; Mosallam et al., 2015). For different researches, Elsanadedy et al. (2013) have used a maximum element size of 25mm, while Mosallam et al. (2015) have used a maximum element size of 12.5mm. These should be taken only as reference

as mesh convergence test carried out would generate different results for different geometry of RC beams.

To model steel reinforcement, MAT003 (MAT_PLASTIC_KINEMATIC) and MAT024 (MAT_PIECEWISE_LINEAR_PLASTICITY) are recommended in which both require minimum input material properties of steel rebars (Hallquist, 2007).

In case of a symmetrical beam is in interest, it can be modelled only half as theoretically both sides or both half of the beam would behave similarly, even though it is not true in reality. However, as far as finite element analysis is concerned, modelling only half of the beam is extremely beneficial as well in reducing computational time, as there are less elements to be computed. In such cases, symmetry boundary condition is to be defined on nodes on the plane at which the beam is cut into half. For these nodes, restraint conditions are defined such that it will resemble simulation using the full-span beam. Besides, node sets can also be created to define the support as well as the loading point, with certain restraint condition defined on the basis on how the RC beam is modelled in the global coordinates system (Almusallam et al., 2015; Elsanadedy et al., 2013; Mosallam et al., 2015).

CHAPTER 3

METHODOLOGY

3.0 Introduction

The focus of this research is quasi-static simulation comparing two concrete material models available in LS-DYNA material library – MAT159 and MAT072R3, studying flexural and shear behaviour of RC beams. Specimens of RC beams that are designed to fail in flexure and shear are selected for the simulation in order to compare the accuracy and reliability of MAT159 and MAT072R3.

3.1 Single Element Test for Concrete Material Model MAT159

Prior to modelling of RC beams for validation purposes, single element tests are carried out, to study several parameters in order to ensure accuracy and consistency of simulation results. In general point of view, two of the parameters include size of element, as well as loading rate involving displacement-controlled explicit quasi-static simulation. In particular for material model MAT159, parameters including compressive strength, aggregate size, cap retraction option, and recovery options are tested by single element test, to examine how changes of these parameters would affect the behaviour of the concrete model. The model used for single element test is as shown in Figure 3.1, which is a single cube element.

In this context, single element tests are carried out using material model MAT159, with a density of 2400 kg/m^3. Displacement controlled static loading is applied on the top 4 nodes of the cube element, acting in negative Z-direction to simulate compressive loading, while a boundary condition constraining the global Z-displacement direction is defined at the bottom 4 nodes of the cube element. Loading rate is assigned by defining a loading curve with constant velocity, to avoid unnecessary inertia forces and induced acceleration. A solid section is also assigned

to the concrete cube element. Hourglass energy calculation is also enabled to monitor the overall stability of the single element model. After several preliminary testing, the following methodologies as follow are adopted for the miscellaneous single element tests.

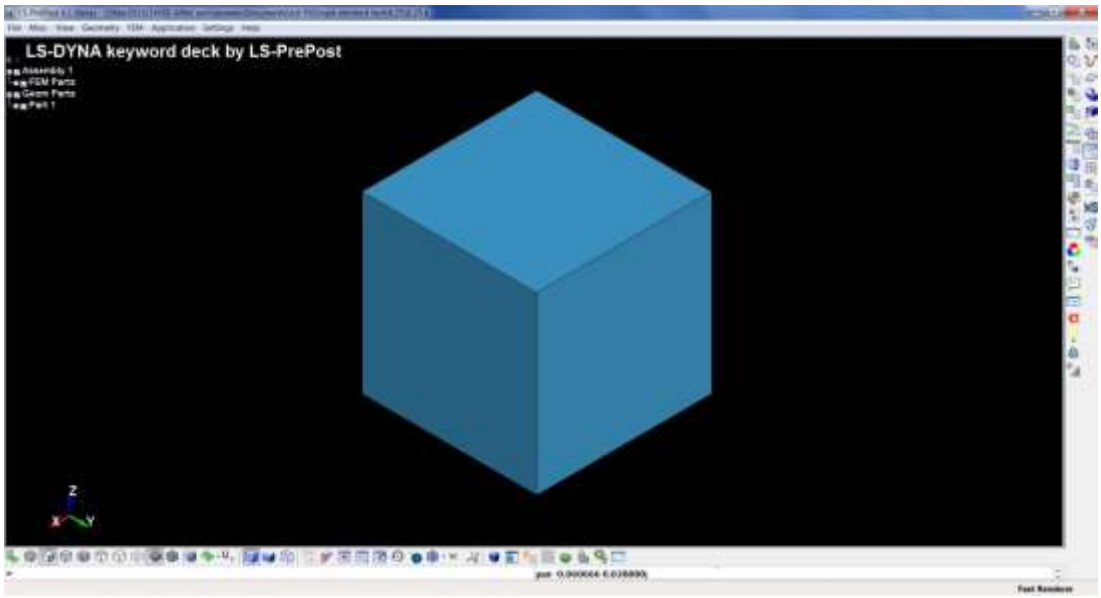

Figure 3.1: Model used for single element test using LS-DYNA.

3.1.1 Size of Element

Several sizes of element are being tested in single element test, which include element sizes of 1mm, 6.25mm, 10mm, 12.5mm, 25mm, and 50mm. Note that the element sizes as mentioned are dimensions of the single cube element in each single element test. These are tested with concrete with 30MPa of compressive strength, 19mm of aggregate size, loading rate of 1mm/s, as well as default options for both cap retraction option and recovery option (IRETRC=0 & RECOV=0).

3.1.2 Quasi-static Loading Rate

Single element test is carried out using displacement controlled static loading rate of 0.1mm/s, 1mm/s, 5mm/s, and 10mm/s, with 30MPa of concrete compressive strength, 19mm of aggregate size, element size of 25mm, as well as default options for both cap retraction option and recovery option (IRETRC=0 & RECOV=0).

3.1.3 MAT159 – Compressive Strength

Compressive strength of concrete is studied by running the single element test using compressive strengths of 18MPa, 20MPa, 25MPa, 28MPa, 30MPa, 35MPa, and 38MPa. Other parameters are set constant, such that aggregate size as 19mm, element size as 25mm, loading rate as 1mm/s, as well as default options for both cap retraction option and recovery option (IRETRC=0 & RECOV=0).

3.1.4 MAT159 – Aggregate Size

Effect of aggregate sizes has on the behaviour of concrete model is studied using aggregate sizes of 8mm, 12.5mm, 19mm, 25mm, and 32mm. The remaining parameters are kept constant, with compressive strength of 30MPa, loading rate of 1mm/s, element size of 25mm, as well as default options for both cap retraction option and recovery option (IRETRC=0 & RECOV=0).

3.1.5 MAT159 – Cap Retraction Option

Cap retraction option is studied using default option (IRETRC=0) in which the cap (as shown in Figure 2.4) does not retract, and IRETRC=1 in which the cap retracts. Other parameters are set constant as 30MPa compressive strength, 19mm aggregate size, loading rate of 1mm/s, element size of 25mm, as well as default options for recovery option (RECOV=0).

3.1.6 MAT159 – Recovery Option

Recovery option is associated with the post-damage elastic modulus of the concrete model. This option is studied using default option – RECOV=0 (modulus is recovered in compression), and RECOV=1 (modulus remains at brittle damage level), in which these two definitions are associated with recovery based on sign of pressure invariant only. Also, recovery option is studied using RECOV=10 and

RECOV=11, which both are associated with sign of pressure and volumetric strain. Partial damage recovery can be simulated by defining a value between 0 and 1, or between 10 and 11, for RECOV option (Hallquist, 2007). Other parameters are set constant as 30MPa compressive strength, 19mm aggregate size, loading rate of 1mm/s, element size of 25mm, as well as default options for cap retraction option (IRETRC =0).

3.2 Single Element Test for Concrete Material Model MAT072R3

The same single element test is carried out to investigate the response of MAT072R3. The effects of size of element and loading rate on behaviour of the single cube element are also studied. Details are as of Section 3.1.1 and 3.1.2, respectively. Input parameters of MAT072R3 such as unconfined compressive strength (A0) and aggregate size (LOCWIDTH) are tested as well. To study the effect of compressive strength and aggregate size on stress-strain behaviour of the single element cube, testing mechanism is the similar to MAT159, as stated in Section 3.1.3 and 3.1.4 respectively. Important point to note is that unconfined compressive strength shall be input as a negative value, representing compression strength of concrete. In addition to this, LOCWIDTH is specified as three times the maximum aggregate diameter.

3.3 Validation of Modelling Techniques

Owing to the modelling techniques used in this research, two validation works are done in order to ensure that FE results will remain consistent regardless of the modelling techniques. These validations include half beam modelling and modelling using node set vs cylinder for support and load application.

3.3.1 Half Beam Modelling

It should be noted that half beam modelling is only applicable to symmetrical beams. Half beam modelling is done on the basis of the theory such that when a RC beam is

symmetry in nature and is loaded symmetrically, the reaction and behaviour on both sides of the RC beams should be similar, even though the experimental works, often, showed otherwise. A node set is created at the mid span of the beam at which the modelled beam is cut into half, consisting of all the associated nodes on the face. A symmetry boundary is then defined to simulate a full beam condition using the half beam model. Geometry and testing mechanism of the selected beam are as shown in Figure 3.2 is used for validation of half beam modelling.

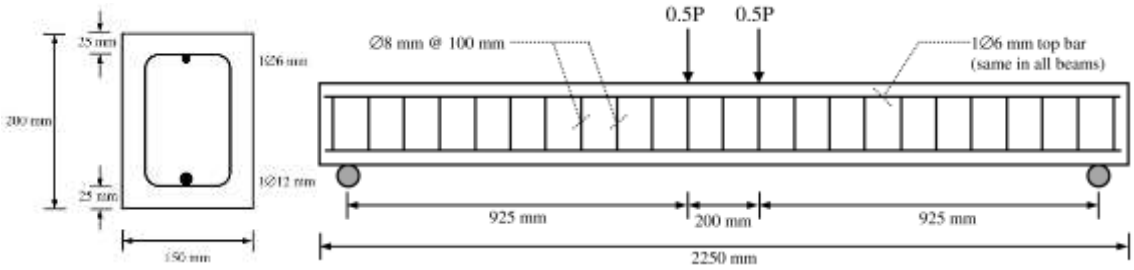

Figure 3.2: Geometry and testing mechanism of B1Ø12 by Almusallam et al. (2015).

Finite element (FE) modelling of the RC beam used for validating half beam modelling is done based on the material properties and relevant conditions as shown in Table 3.1. The results generated from the half beam model with symmetry boundary condition will eventually be compared to that of the full beam model to ensure that half beam modelling is acceptable, both models are shown in Figure 3.3 and Figure 3.4. Results such as the behaviour of the model and load-deflection curve of the models are compared.

Table 3.1: Material Properties and Relevant Information Defined in FE Modelling of RC Beam Tested for Validation of Half Beam Modelling (Almusallam et al., 2015)

Material Properties		
Material	**Properties**	**Values**
Concrete	Material model	MAT159 (MAT_CSCM_CONCRETE)
	Density (kg/m^3)	2,320
	Uniaxial compressive strength (MPa)	28
	Maximum aggregate size (mm)	10
	ERODE	1.05
	RECOV	0
	ITRETRC	0

Steel rebars	Bar diameter (mm)	Top rebar Ø6	Bottom rebar Ø12	Stirrup Ø8
	Material model	MAT024 (MAT_PIECEWISE_LINEAR_PLASTICITY)		
	Density (kg/m^3)	7,850		
	Young's modulus (GPa)	200		
	Poisson's ratio	0.3		
	Yield stress (MPa)	280	553	493
	Tangent modulus (MPa)	463	785	468
	Plastic strain to failure (%)	19.8	11.7	11.7
Relevant Information				
Element Size		12.5 mm*		
Quasi-static Loading Condition		10 mm/s		
Symmetry Boundary Condition		Full Beam	None	
		Half Beam	Restraint DZ, RX, RY	

* Three dimensions of each element are modelled as close to 12.5mm as possible

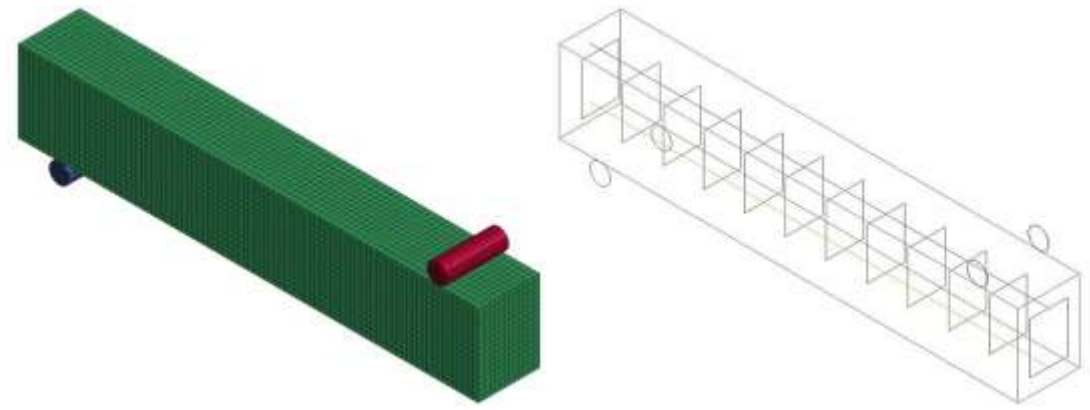

Figure 3.3: Half beam model modelled for validation of half beam modelling.

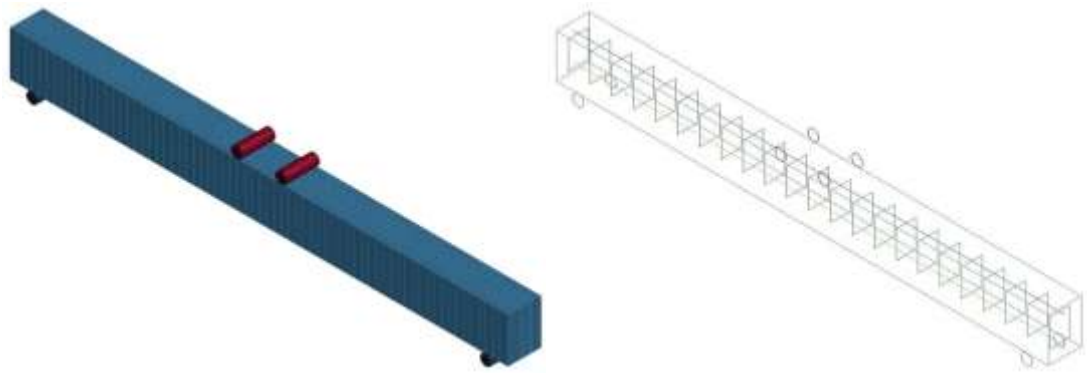

Figure 3.4: Full beam model modelled for validation of half beam modelling.

3.3.2 Modelling Using Node Set vs Cylinder for Support and Load Application

To serve as a point for support and load application, a solid cylinder can be modelled at the desired location, similar to that used in a laboratory experimental mechanism. However, Almusallam et al. (2015) suggested using a node set consisting of nodes at the support location as well as at the load application location, subsequently assigning boundary condition to the support node set and prescribed motion to the load application node set. Results shown that simulation using node set can correlate well to the experimental results too (Almusallam et al., 2015).

To carry out validation of this modelling technique, control beam by Teo & Lau (2015) is adopted. Geometry and testing mechanism of control beam B1 by Teo & Lau is as shown in Figure 3.5. FE modelling of the RC beam is done according to the material properties and other relevant conditions as shown in Table 3.2. The FE models are as follow, as shown in Figure 3.6 and 3.7.

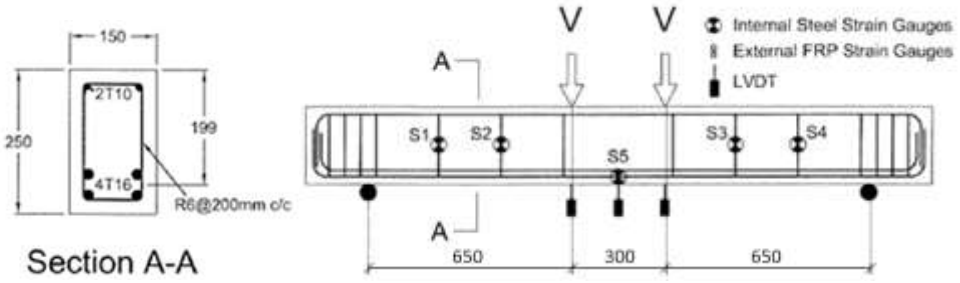

Figure 3.5: Geometry and testing mechanism of control beam B1 by Teo & Lau (2015).

Table 3.2: Material Properties and Relevant Information Used in Finite Element Modelling of B1 Control Beam (Teo & Lau, 2015)

Material Properties		
Material	**Properties**	**Values**
Concrete	Material model	MAT072R3 (MAT_CONCRETE_DAMAGE_REL3)
	Density (kg/m^3)	2,400
	Uniaxial compressive strength (MPa)	22.73
	Maximum aggregate size (mm)	20
	ERODE	1.05
	RECOV	0

	ITRETRC	0		
Steel rebars	Bar diameter (mm)	Top rebar Ø10	Bottom rebar Ø16	Stirrup Ø6
	Material model	MAT003 (MAT_PLASTIC_KINEMATIC)		
	Density (kg/m^3)	7,850		
	Young's modulus (GPa)	200		
	Poisson's ratio	0.3		
	Yield stress (MPa)	412.7	622.5	250
	Tangent modulus (MPa)	-	-	-
	Plastic strain to failure (%)	-	-	-
Relevant Information				
Element Size		25 mm*		
Quasi-static Loading Condition		1 mm/s		
Symmetry Boundary Condition		Half Beam	Restraint DZ, RX, RY	

* Three dimensions of each element are modelled as close to 25mm as possible.

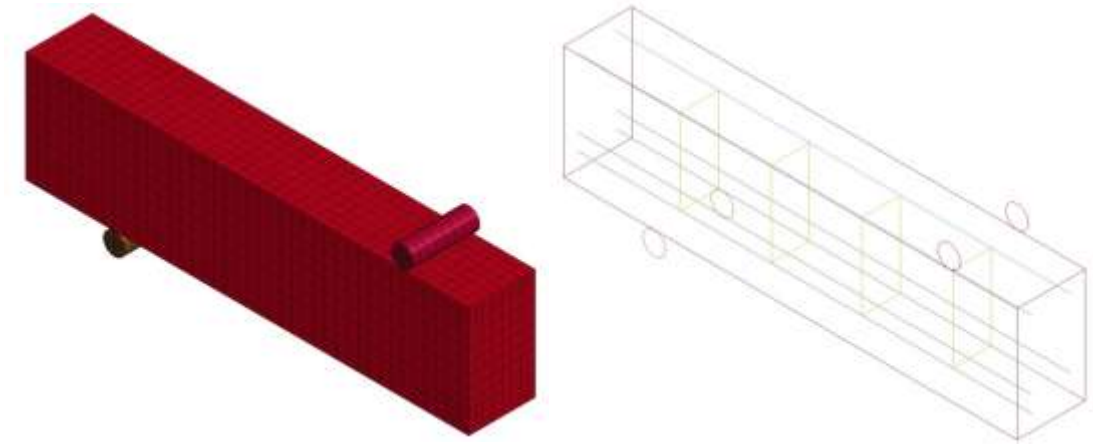

Figure 3.6: Model of control beam B1 using cylinders for support and load application.

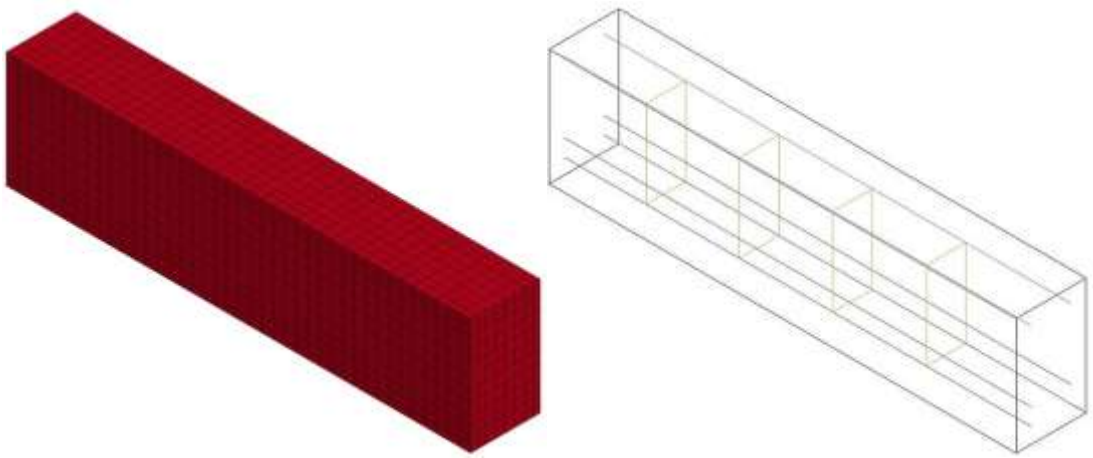

Figure 3.7: Model of control beam B1 using node sets for support and load application.

3.4 Comparative Study between MAT159 and MAT072R3 on Flexural Behaviour Study of RC Beams

3.4.1 B-1Ø12, B-2Ø12, and B-3Ø12 by Almusallam et al. (2015)

Three RC beams by Almusallam et al. (2015) are used to compare MAT159 and MAT072R3. Geometry of the three control beams is shown in Figure 3.8.

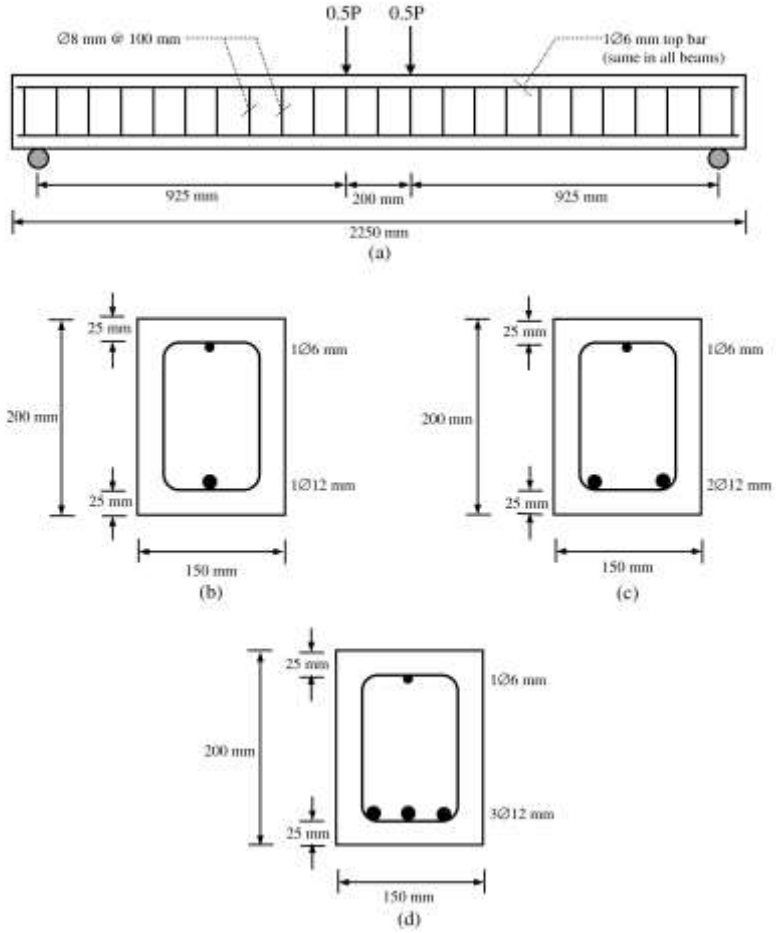

Figure 3.8: Geometry and testing mechanism of B-1Ø12, B-2Ø12, and B-3Ø12 (Almusallam et al., 2015)

Note that the aim of this study by Almusallam et al. (2015) is to study the flexural behaviour of RC beams. All beams as shown are designed to fail in flexure. FE modelling of the three RC beams is done according to the material properties and other relevant conditions as shown in Table 3.3. The difference between the three RC beams is the number of compression steel bars they have, in which B-1Ø12 has one bar, B-2Ø12 has two bars, and B-3Ø12 has three bars, as shown in Figure 3.8. The FE models (half beam models) are as follow, as shown in Figure 3.9, Figure 3.10 and Figure 3.11.

Table 3.3: Material Properties and Relevant Information Defined in FE Modelling of RC Beam Tested for Validation of Half Beam Modelling (Almusallam et al., 2015)

Material Properties				
Material	**Properties**	**Values**		
Concrete	Material model	MAT159 (MAT_CSCM_CONCRETE) MAT072R3 (MAT_CONCRETE_DAMAGE_REL3)		
	Density (kg/m^3)	2,320		
	Uniaxial compressive strength (MPa)	38		
	Maximum aggregate size (mm)	10		
	ERODE	1.05		
	RECOV	0		
	ITRETRC	0		
Steel rebars	Bar diameter (mm)	Top rebar Ø6	Bottom rebar Ø12	Stirrup Ø8
	Material model	MAT024 (MAT_PIECEWISE_LINEAR_PLASTICITY)		
	Density (kg/m^3)	7,850		
	Young's modulus (GPa)	200		
	Poisson's ratio	0.3		
	Yield stress (MPa)	280	553	493
	Tangent modulus (MPa)	463	785	468
	Plastic strain to failure (%)	19.8	11.7	11.7
Relevant Information				
Element Size		10 mm*		
Quasi-static Loading Condition		10 mm/s		
Symmetry Boundary Condition		Full Beam	None	
		Half Beam	Restraint DZ, RX, RY	

* Three dimensions of each element are modelled as close to 10mm as possible

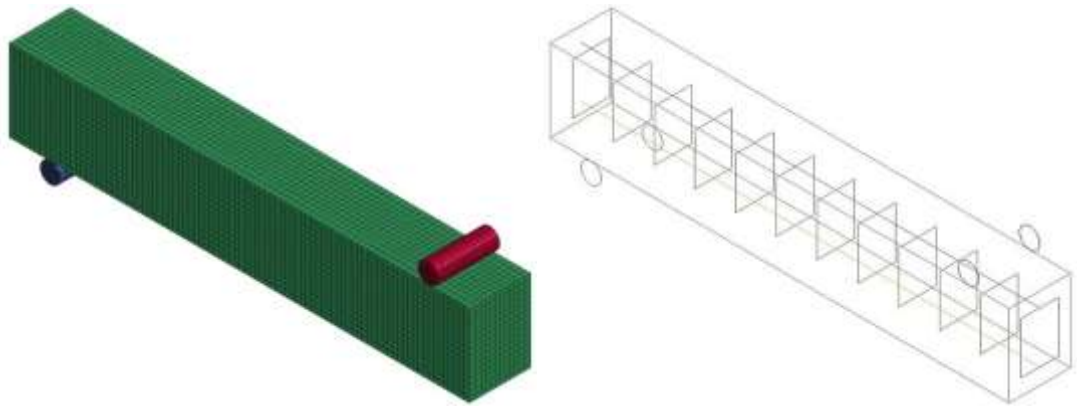

Figure 3.9: Half beam model of B-1Ø12 in LS-DYNA.

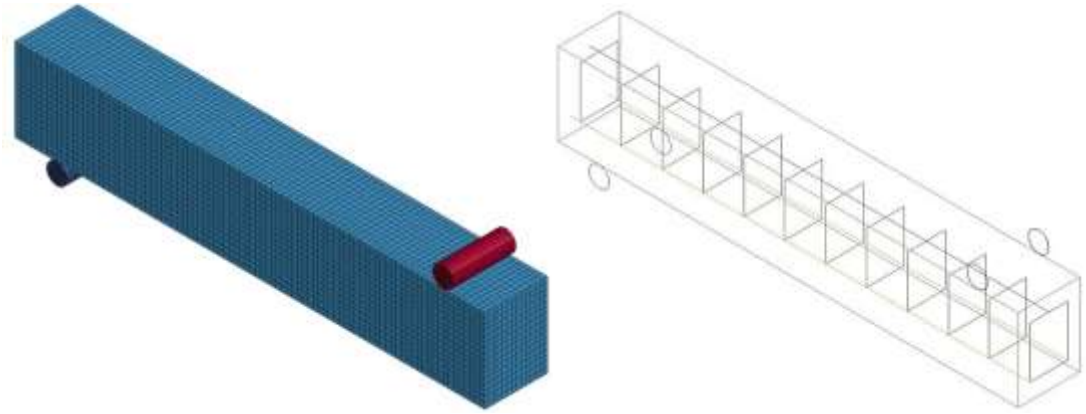

Figure 3.10: Half beam model of B-2Ø12 in LS-DYNA.

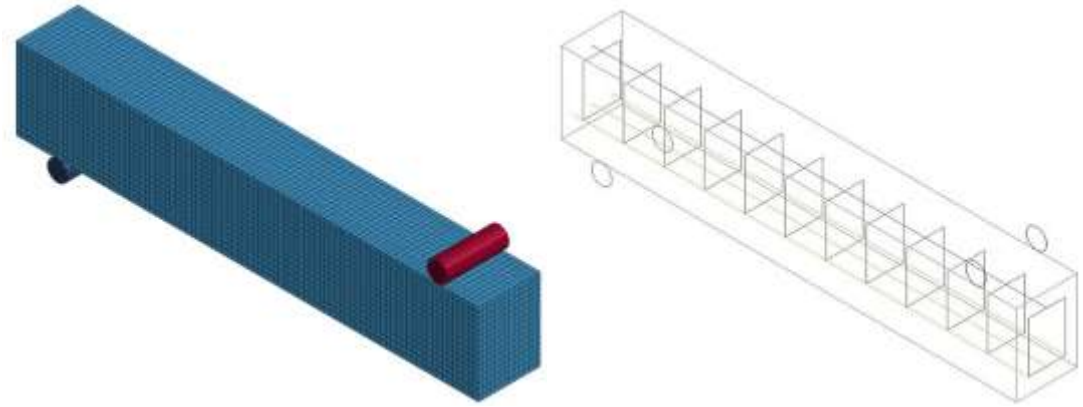

Figure 3.11: Half beam model of B-3Ø12 in LS-DYNA.

3.5 Comparative Study between MAT159 and MAT072R3 on Shear Behaviour Study of RC Beams

In addition to flexural behaviour of RC beams, shear behaviour of RC beams modelled using MAT159 and MAT072R3 is also of interest. Therefore, control beams by Teo & Lau (2015) and Zhang & Hsu (2005) are referenced to study MAT159 and MAT072R3 for RC beams under quasi-static loading, as they are designed to fail in shear.

3.5.1 B1 Control Beam by Teo & Lau (2015)

Geometry and testing mechanism of control beam B1 are shown in Figure 3.5. FE modelling of the RC beam by Teo & Lau (2015) is done according to the material properties and other relevant conditions as shown in Table 3.2. The FE model is as shown in Figure 3.6.

3.5.2 ZC4, ZC6, and ZC6(2) by Zhang & Hsu (2005)

Three control beams, ZC4, ZC6, and ZC6(2) by Zhang & Hsu (2005) are as shown in Figure 3.12, 3.13, and 3.14 respectively.

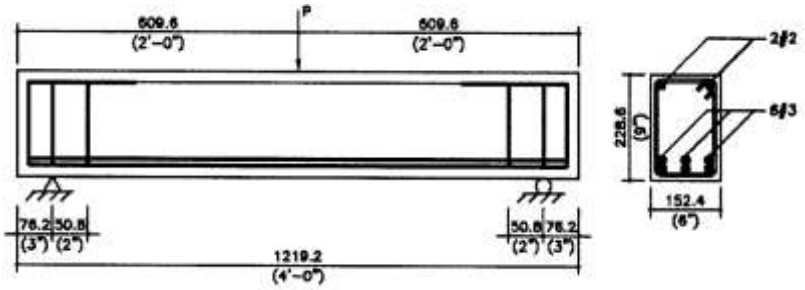

Figure 3.12: Geometry and testing mechanism of ZC4 by Zhang & Hsu (2005).

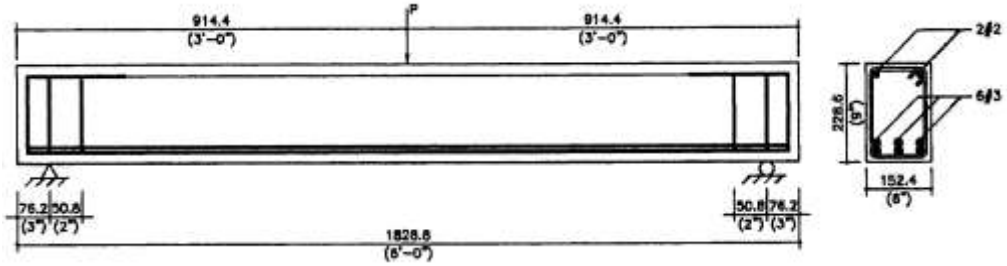

Figure 3.13: Geometry and testing mechanism of ZC6 by Zhang & Hsu (2005).

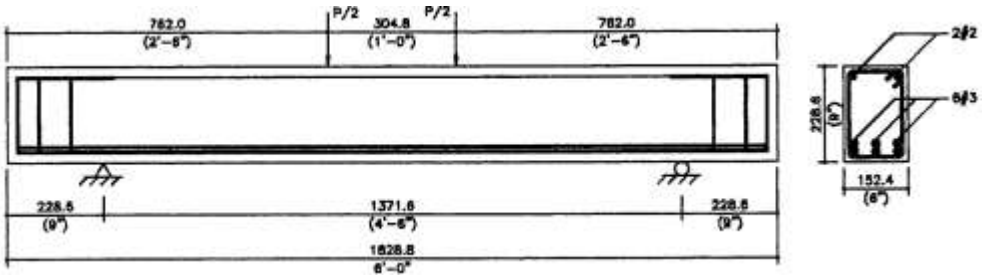

Figure 3.14: Geometry and testing mechanism of ZC6(2) by Zhang & Hsu (2005).

Material properties and relevant information used in FE modelling of ZC4, ZC6, and ZC6(2) are shown in Table 3.3. FE models generated in LS-DYNA are shown in Figure 3.15, 3.16, and 3.17 respectively.

Table 3.4: Material Properties and Relevant Information Used in Finite Element Modelling of ZC4, ZC6, and ZC6(2) Control Beams (Zhang & Hsu, 2005)

Material Properties		
Material	**Properties**	**Values**
Concrete	Material model	MAT159 (MAT_CSCM_CONCRETE) MAT072R3 (MAT_CONCRETE_DAMAGE_REL3)
	Density (kg/m^3)	2,400
	Uniaxial compressive strength (MPa)	43.862
	Maximum aggregate size (mm)	9.5
	ERODE	1.05
	RECOV	0
	ITRETRC	0
Steel rebars	Bar diameter (mm)	Bottom rebar #3 (=9.5mm)
	Material model	MAT003 (MAT_PLASTIC_KINEMATIC)
	Density (kg/m^3)	7,850
	Young's modulus (GPa)	200
	Poisson's ratio	0.3
	Yield stress (MPa)	399.62
	Tangent modulus (MPa)	-
	Plastic strain to failure (%)	-
Relevant Information		
Element Size	25 mm*	
Quasi-static Loading Condition	1 mm/s	
Symmetry Boundary Condition	Half Beam	Restraint DZ, RX, RY

* Three dimensions of each element are modelled as close to 25mm as possible

Note that the top bars are not modelled as these bars serve as a point of attachment to keep the stirrups at both sides on the beam in place.

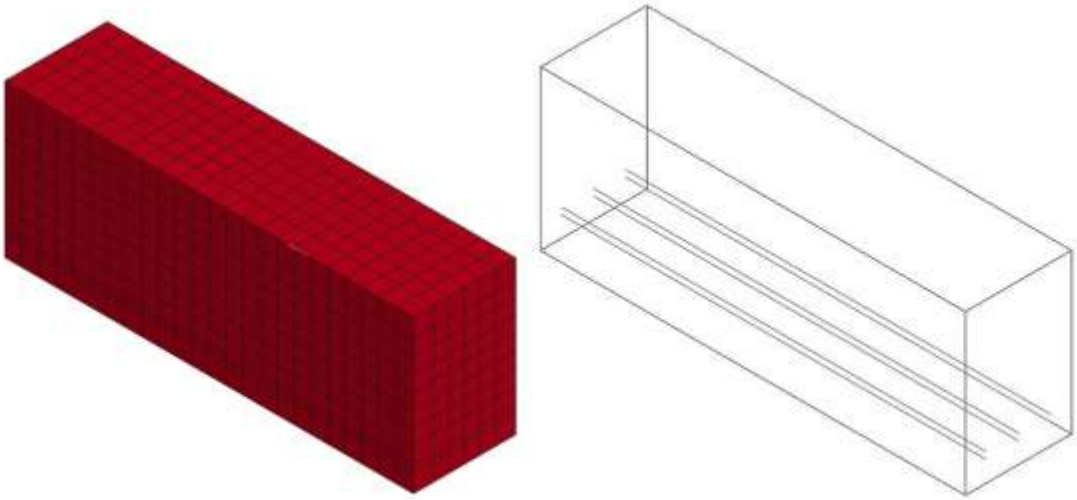

Figure 3.15: FE model of ZC4.

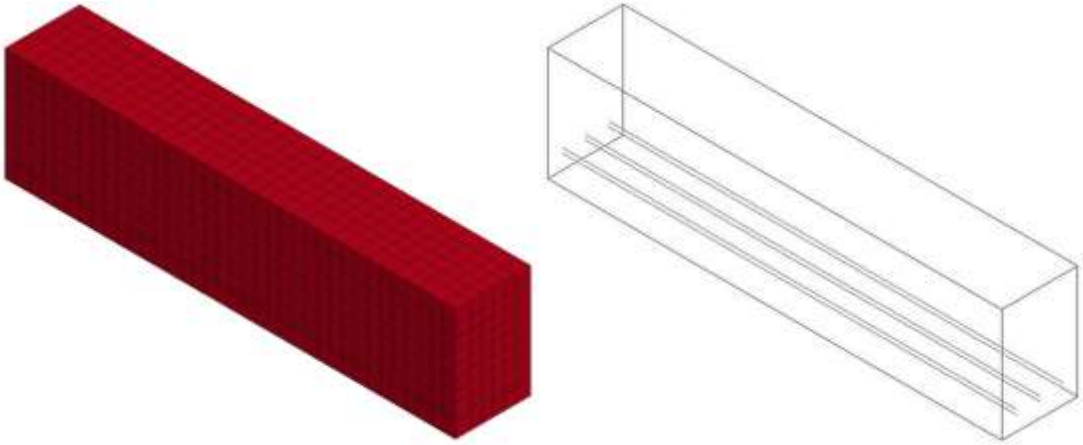

Figure 3.16: FE model of ZC6 and ZC6(2).

Models of ZC6 and ZC6(2) seem the same, as shown in Figure 3.16, but the location of support and load application differs, defined according to Figure 3.13 and 3.14.

3.6 Calibration of LS-DYNA Model for Concrete Material Model MAT072R3

As several input parameters of MAT159 are studied using single element test, some input parameters are studied using a RC beam model, which are important for calibration of FE results. Calibration of LS-DYNA model is done so that appropriate adjustment of input parameters with good engineering judgement can be made in order to simulate the actual behaviour of RC beams tested in the laboratory. Some

adjustments might need additional information from the laboratory tests, while some adjustments are associated with equations and thereafter deduced by using relevant parameters.

Specifically for MAT072R3, two input parameters are studied for calibration purposes. These include the uniaxial tensile strength (FT), and three times the maximum aggregate diameter (LOCWIDTH). In addition to this, modulus of elasticity of the concrete material model can also be adjusted, however, not in a direct way. In this context, an Equation-of-State (EOS), namely EOS_TABULATED_COMPACTION can be defined in terms of pressure-volumetric strain response, which represents the bulk modulus, *K*, thus modulus of elasticity, *E*, by the equation as follows, where *v* is Poisson's ratio.

$$E = \frac{dP}{d\varepsilon_V} = 3K(1 - 2v)$$

Prior to defining EOS, all input parameters in MAT072R3 are input in order for the defined EOS to be taken into account in computation. Else, EOS will be auto-generated according to the compressive strength, superseding the defined EOS.

3.6.1 MAT072R3 – Uniaxial Tensile Strength (FT)

Tensile strength of concrete is often assumed as approximately 10% of its compressive strength, as a rule of thumb. FT self-generated in LS-DYNA conforms to this rule of thumb too. However, in case of concrete with higher tensile strength is used, FT can be specified by user. In this research, a simple test is carried out, using control beam B1 by Teo & Lau (2015), by increasing the FT from the one auto-generated by LS-DYNA. Unconfined compressive strength of concrete is 22.73MPa. Testing mechanism is as shown below. Note that this test is solely to study the effect of FT on behaviour of RC beam in terms of load-deflection curve.

Table 3.5: Testing mechanism of effect of FT on behaviour of RC beam

Test #	FT
1 (Default)	2.413 MPa
2	3.413 MPa
3	4.413 MPa

3.6.2 MAT072R3 – LOCWIDTH

LOCWIDTH is an input parameter which requires user to specify as three times the maximum aggregate size. By default, the self-generated value of LOCWIDTH is set as 25.4mm. A similar test is thereby done using control beam B1 by Teo & Lau (2015) as well to study the effect of maximum aggregate size on the behaviour of RC beam under quasi-static loading. Testing mechanism is as shown below.

Table 3.6: Testing mechanism of effect of LOCWIDTH on behaviour of RC beam

Test #	Maximum Aggregate Size	LOCWIDTH
1	5mm	15mm
2 (Default)	8.47mm	25.4mm
3	10mm	30mm
4	15mm	45mm
5	20mm	60mm
6	25mm	75mm

3.6.3 MAT072R3 – Modulus of Elasticity

Modulus of elasticity of concrete model MAT072R3 can be adjusted by specifying the second value of pressure, which is represented by C2 in the keyword EOS_TABULATED_COMPACTION, in which the corresponding volumetric strain (EV2) is -0.0015 by default, as shown in Figure 3.17. The input parameters highlighted with red boxes as shown are to be modified in case of adjustment of modulus of elasticity of concrete is required. K1 and K2 represent the unloading bulk modulus, which corresponds to the specified values of pressure and volumetric strain. Testing is done using control beam B1 by Teo & Lau (2015) and the testing mechanism is as shown in Table 3.6.

Table 3.7: Testing mechanism of effect of C2 on behaviour of RC beam

Test #	Pressure C2 (GPa)	Volumetric Strain EV2	Unloading Bulk Modulus K1 & K2 (GPa)
1	0.0088	-0.0015	5.87
2 (Default)	0.0188	-0.0015	12.53
3	0.0288	-0.0015	19.2

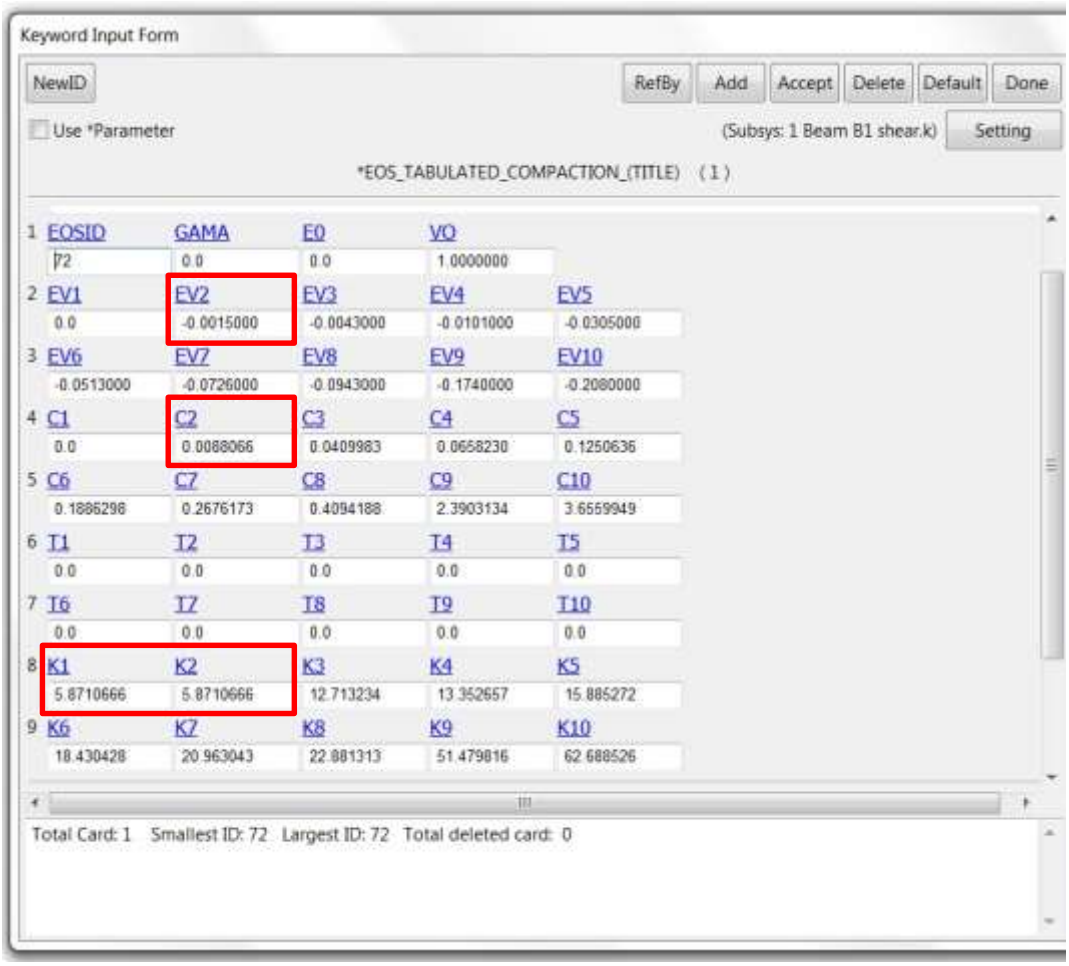

Figure 3.17: The EOS_TABULATED_COMPACTION keyword input form specifying the input parameters to be modified to adjust the modulus of elasticity of concrete material model MAT072R3.

3.7 Gantt Chart / Project Milestones

No.	Activities	Week No.																									
		FYP I														FYP II											
		1	2	3	4	5	6	7	8	9	10	11	12	13	14	1	2	3	4	5	6	7	8	9	10	11	12	13	14
1	Selecting FYP project topic																												
2	Development of literature review																												
3	Start of simulation works			◆																									
4	Getting familiar with LS-DYNA																												
5	Comparative study between MAT159 and MAT072R3 on flexural behaviour of RC beam																												
6	Comparative study between MAT159 and MAT072R3 on shear behaviour of RC beam																												
9	Results and discussion																												
10	End of simulation works																												◆

Process

◆ Milestone

CHAPTER 4

RESULTS & DISCUSSION

4.0 Introduction

In this section, results generated from LS-DYNA are presented. For single element tests, results presented include the stress-strain diagram of the single cube element due to the displacement controlled static loading applied to the cube element. For comparative studies between MAT159 and MAT072R3, results such as behaviour of the RC beams, precisely the effective plastic strain of the elements, as well as load-deflection curves are presented. Load-deflection curves generated from LS-DYNA are compared to those of experimental works or those as presented in research papers.

4.1 Single Element Tests for Concrete Material Model MAT159

4.1.1 Size of Element

Figure 4.1 shows the stress-strain diagram of the single element test in comparison of the sizes of element, including 1mm, 6.25mm, 10mm, 12.5mm, 25mm, and 50mm.

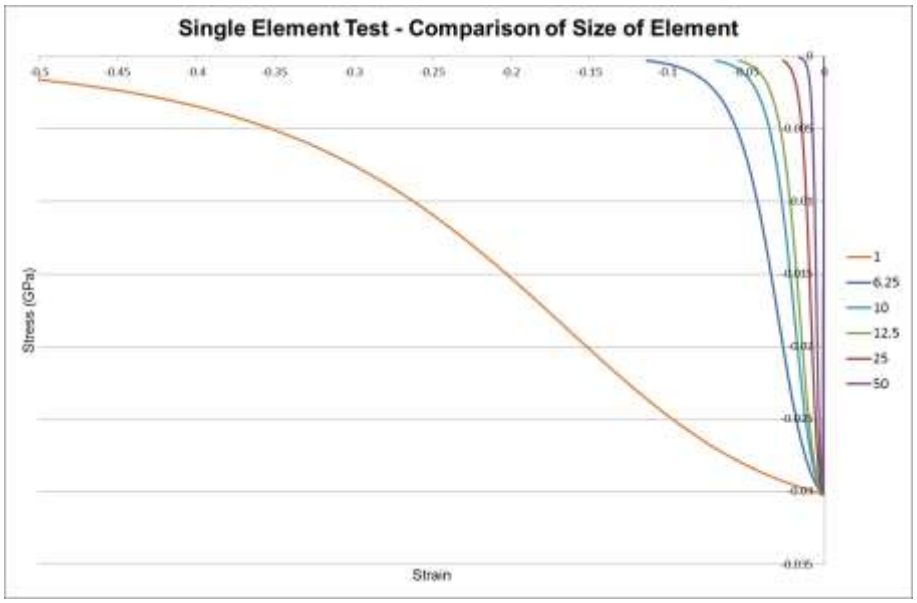

Figure 4.1: Stress-strain diagram of single element test studying the effect of element size.

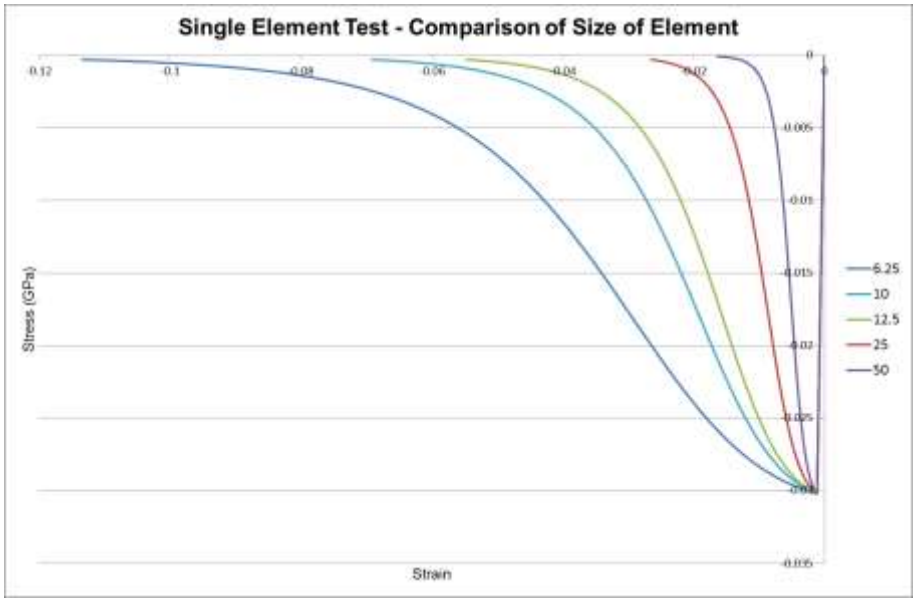

Figure 4.2: Stress-strain diagram of single element test studying the effect of element size, without the results of element size of 1mm.

The stress-strain diagram has shown that size of element has no effect on the pre-failure behaviour of the element, which has shown a linear stress-strain behaviour until it reaches its unconfined compressive strength, in this case, 30MPa. Post-failure behaviour of the concrete element has shown that the greater the size of element, the stiffer the element is which yielded a lower plastic strain as the amount of material resisting the compressive forces is greater.

In case of modelling a RC beam for simulation purposes, this result, however, does not justify which size of element is to be used. It depends on the section properties and longitudinal properties of the particular RC beams to be tested. As such, mesh convergence tests are to be done for each RC beam so as to determine the optimum size of element that should be modelled in order to obtain an adequately converged result yet optimizing the computational time.

4.1.2 Quasi-static Loading Rate

Figure 4.3 shows the stress-strain diagram of single element test, involving tests using loading rate of 0.1 mm/s, 1mm/s, 5mm/s, as well as 10mm/s. These tests are done on a basis such that constant velocity is to be employed so as to avoid

unnecessary inertia forces and acceleration, which could turn the problem into a dynamic condition. However, the constant velocity to be applied is the governing factor of computational time. Thus, to optimize computational time, an adequately gradual loading rate of the beam is to be used.

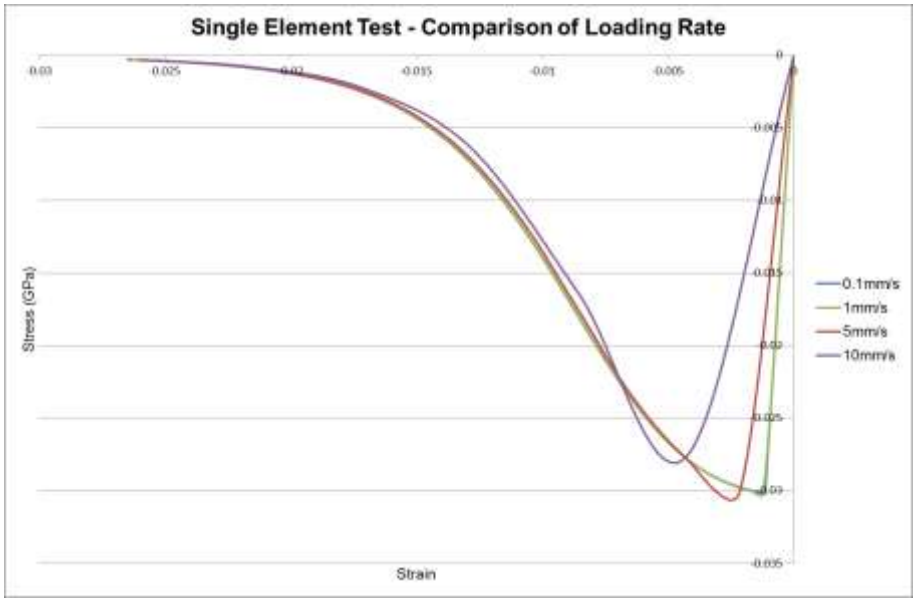

Figure 4.3: Stress-strain diagram of single element test involving various loading rate.

Results showed that 1 mm/s is the optimum quasi-static displacement controlled loading rate to be used in LS-DYNA modelling, as it has shown minimal difference as compared to the more gradual loading rate – 0.1 mm/s. Therefore, subsequent simulation testing will be done using 1 mm/s.

4.1.3 MAT159 – Compressive Strength

As stated by Murray (2007) and Murray et al. (2007), material model MAT159 is appropriate to be used for normal strength concrete ranging from 20MPa to 58MPa, with emphasis on the mid-range of 28MPa to 48MPa. This can be explained and seen rather clear, especially for concrete below the strength of 28MPa, as shown in Figure 4.4.

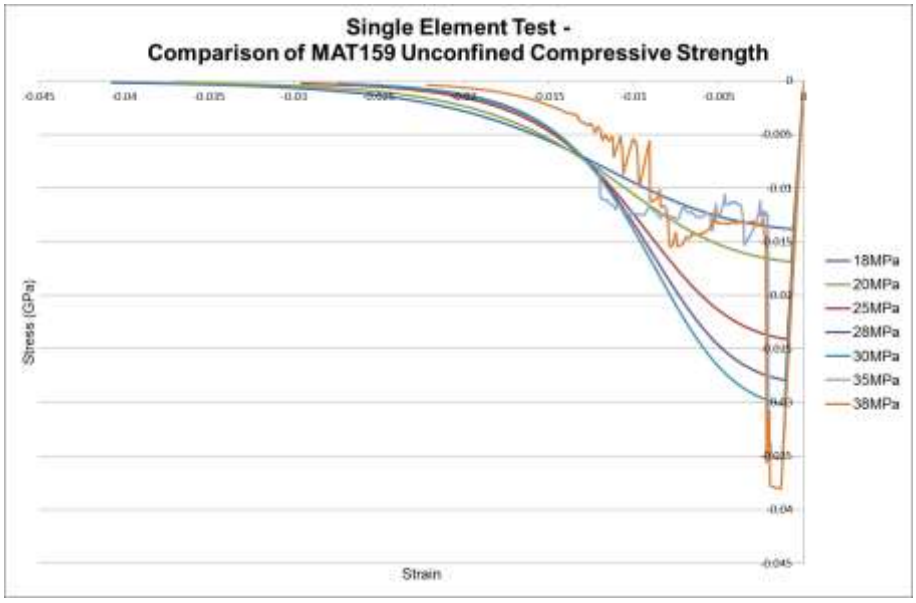

Figure 4.4: Stress-strain diagram comparing concrete model with various unconfined compressive strength.

For concrete models below unconfined compressive strength of 28MPa, it can be seen that the concrete element did not reach its defined compressive strength, for instance 18MPa concrete model reached its peak at only 14MPa, and 20MPa concrete model reached its peak at 17MPa. For concrete models with 28MPa and 30MPa, both have well achieved their compressive strengths. However, it should be noted that for concrete models with unconfined compressive strength exceeding 30MPa, i.e. 35MPa and 38MPa, as shown in Figure 4.4, the softening behaviour of the concrete element did not exhibit a smooth decline of strength, as opposed to those below or equal to 30MPa. Yet, these models have reached the defined unconfined compressive strengths.

4.1.4 MAT159 – Aggregate Size

Figure 4.5 shows that for concrete models with varying aggregate size, ranging from 8mm to 32mm, as recommended by Murray (2007) and Murray et al. (2007), the pre-failure behaviour of the elements has no effect due to the different aggregate size. This has conformed to the statement as stated by Murray et al. (2007) where aggregate size has effect on only the softening behaviour of the damage of concrete models, which has exhibited the post-failure behaviour as shown in Figure 4.5.

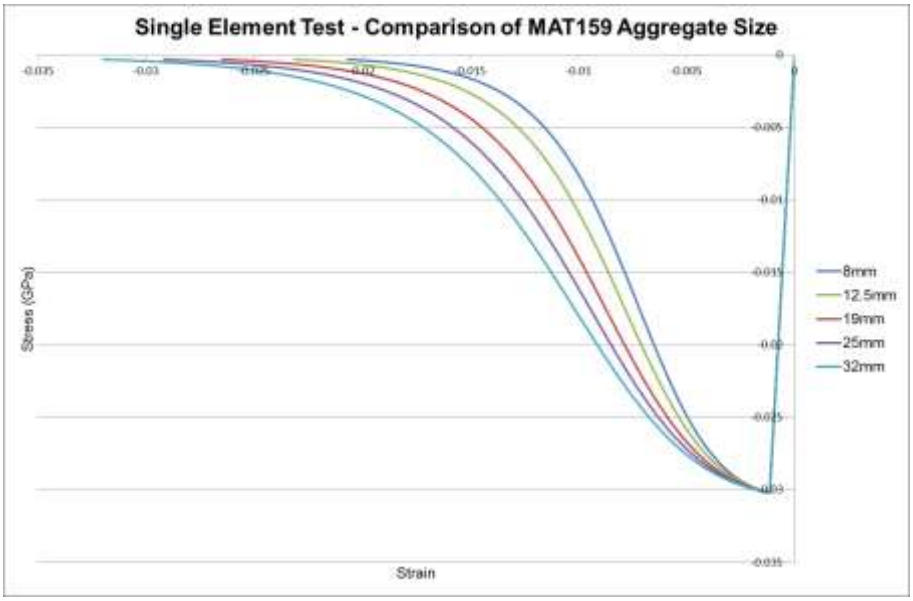

Figure 4.5: Stress-strain diagram of single element tests comparing different aggregate size as defined under the material model MAT159.

It can be seen that the greater the maximum aggregate size, the strength of concrete element drops to zero and soften with a slightly higher strain, which means that the overall concrete element is slightly more deformable.

4.1.5 MAT159 – Cap Retraction Option

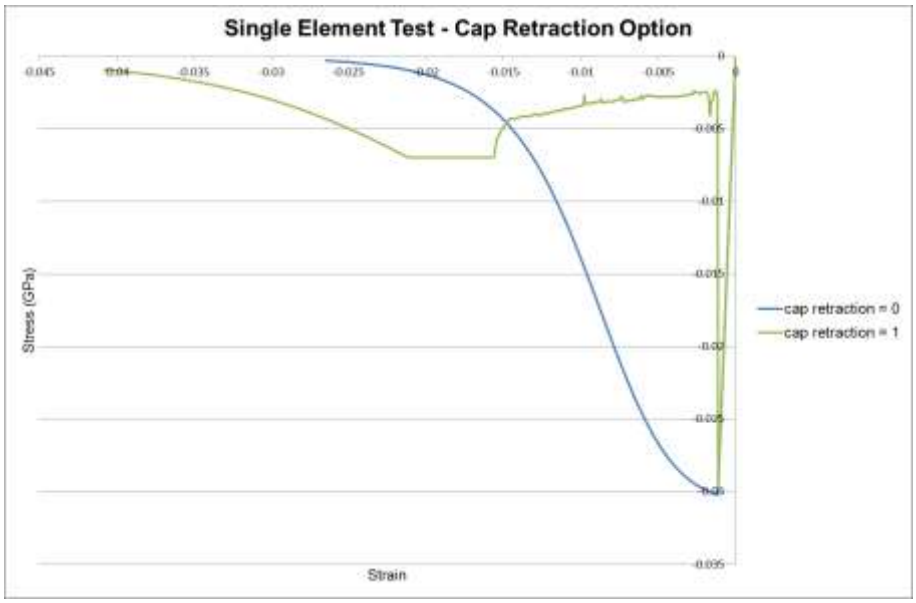

Figure 4.6: Stress-strain diagram of single element test studying the cap retraction option.

Figure 4.6 shows that with cap retraction option turned on, in which the cap model as shown in Figure 2.4 retracts, a sudden drop of strength occurred after the concrete

element reached its unconfined compressive strength. Therefore, it is deduced that cap retraction option should be turned off to simulate the normal softening behaviour of the brittle concrete element.

4.1.6 MAT159 – Recovery Option

Figure 4.7 illustrates that recovery options available for concrete material model MAT159 have no effect on the stress-strain diagram of the single element model. This is because the concrete element is completely loaded compressively. Therefore, using the default option (RECOV=0), in which stiffness of compression is fully recovered from tensile damage when there is a transition from tension to compression for a single element, is to be employed for future simulation, since concrete shown excellent compression properties.

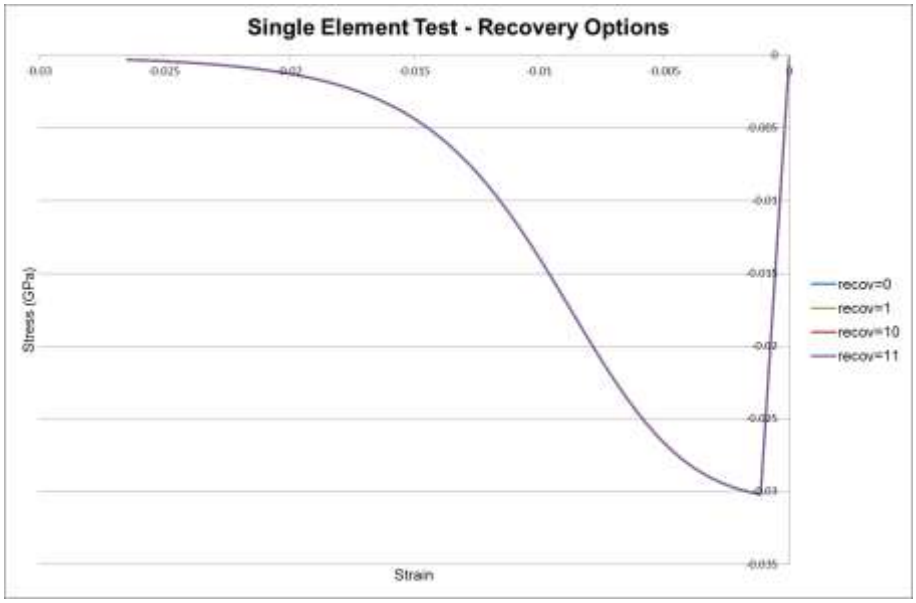

Figure 4.7: Stress-strain diagram of single element test studying recovery options of material model MAT159.

4.2 Single Element Tests for Concrete Material Model MAT072R3

For MAT072R3, it has been found that single element test cannot be carried out to study associated input parameters. This is because the single element model fails at a very low effective stress, which is at 1.77224e-06MPa, for the single element cube that is defined to have 45.4MPa of unconfined compressive strength with loading rate of 2.54mm/s. No solution is found and such behaviour is not explainable. Therefore, the single element test for MAT072R3 is unable to be conducted.

4.3 Validation of Modelling Techniques

4.3.1 Half Beam Modelling

Figure 4.8 and Figure 4.9 depict the comparison between full beam model and half beam model with defined symmetry boundary, in terms of effective plastic strain of control beam B-1Ø12 before the first erosion occurs as well as the load versus mid-span deflection curves of the two models.

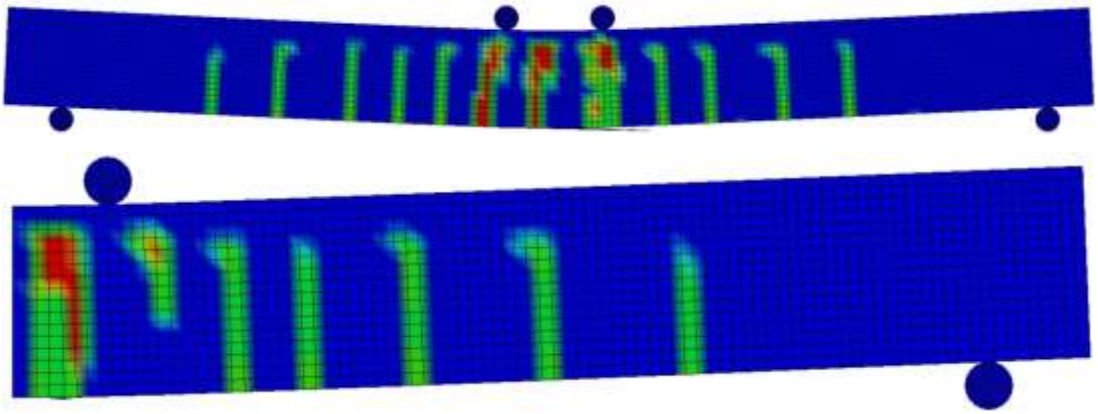

Figure 4.8: Effective plastic strain of RC beams – full beam model (above) and half beam model (below).

Effective plastic strain of the RC beam model can be viewed as cracks that are going to be formed when a beam is loaded. As can be seen in Figure 4.8, both models have shown rather similar effective plastic strain, or cracking pattern.

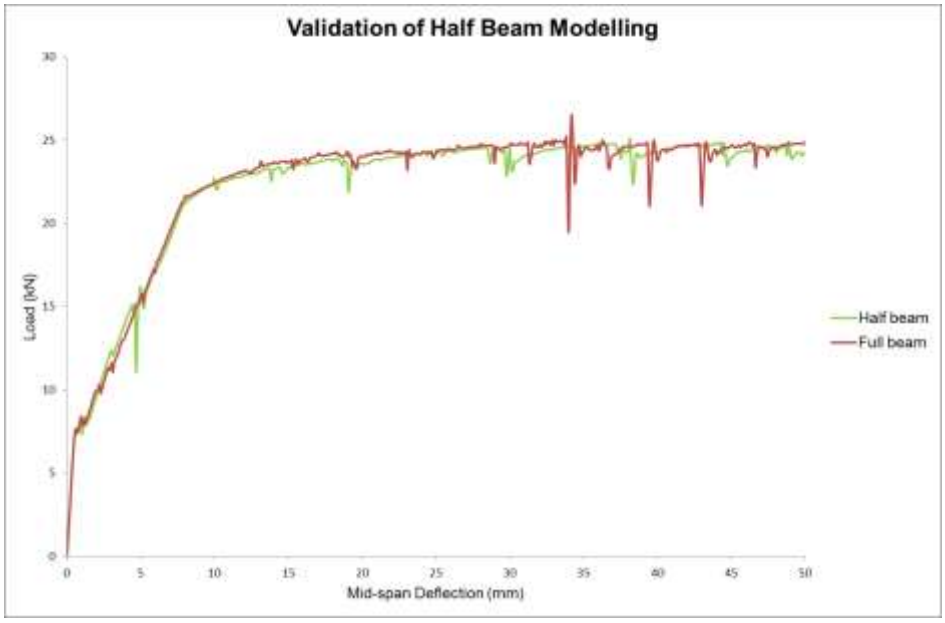

Figure 4.9: Load versus mid-span deflection curves for full beam model and half beam model.

Figure 4.9 has shown that in terms of load-deflection curves, both models have exhibited rather similar behaviour as well, with the initial pre-yielding behaviour which is almost the same. As a result, it is concluded that the half beam model is validated and can be used for subsequent simulation works.

4.3.2 Modelling Using Node Set vs Cylinder for Support and Load Application

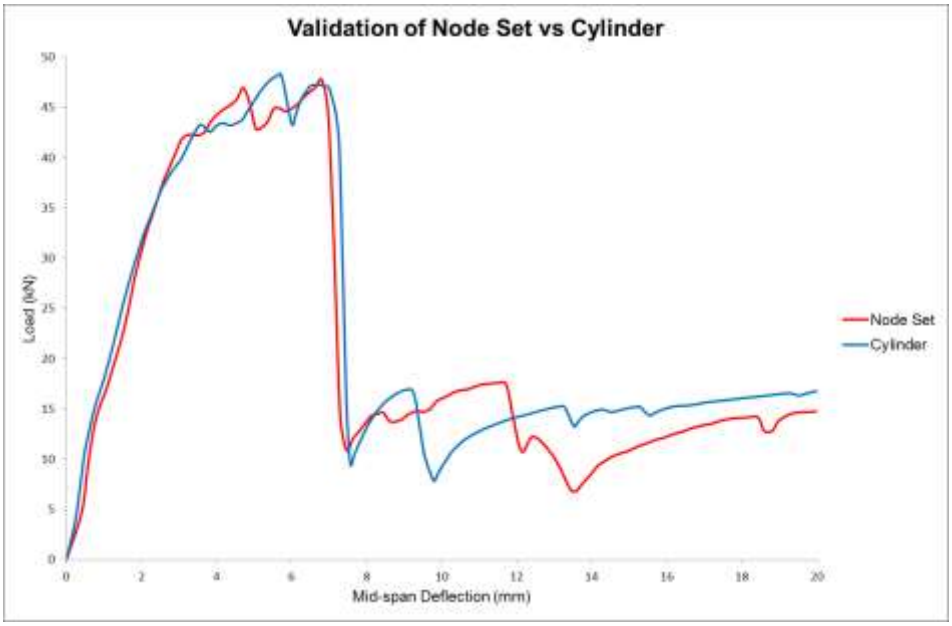

Figure 4.10: Load-deflection curve of validation of using node set versus cylinder for support and load application

Figure 4.10 shows the load-deflection curves of control beam B1, in which the red curve shows the results where load application and support are modelled as node set, while the blue curve shows the case for cylinder. At failure, node set case failed in shear at failure load of 47.75kN while cylinder case failed in shear at failure load of 47.26kN, with a percentage difference of just 1%. Mid-span deflection at failure is 6.808mm for node set case and 6.7mm for cylinder case, with percentage difference of 1.6%. In terms of failure mode, both cases have shown similar results as well. Figure 4.11 and 4.12 shows the time-history d3plot animation of both cases at t=6750ms, where an impression of diagonal shear crack (shown in red) can be seen.

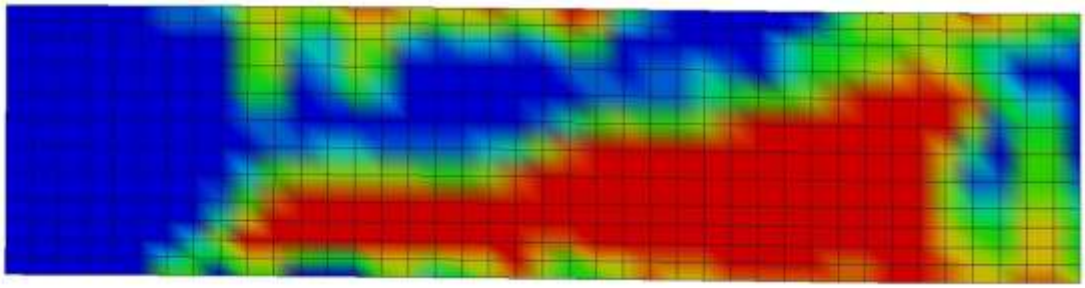

Figure 4.11: Failure mode of control beam B1 with node set as support and medium of load application.

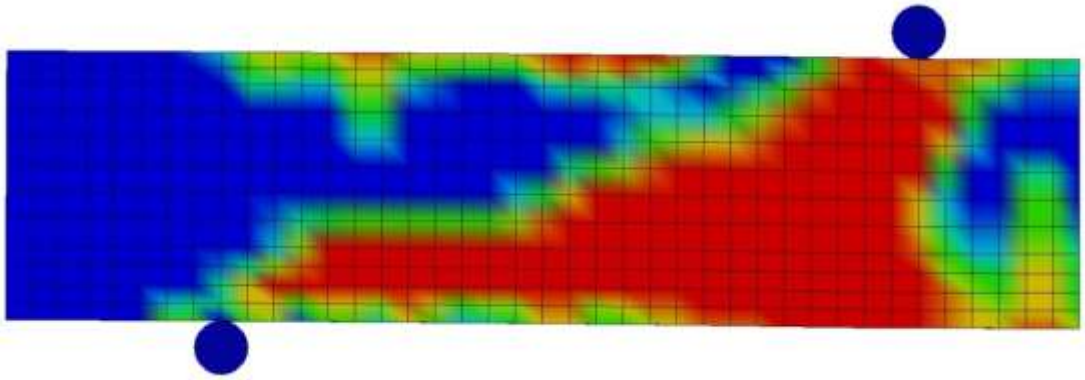

Figure 4.12: Failure mode of control beam B1 with cylinder as support and medium of load application.

It can be deduced that both are applicable in modelling of support and medium of load application for RC beams. This validation test is done due to the occasional instability issue caused by simulation using cylinder for support and load application. Before the RC beam fails, the beam tends to get flung out of the support, causing inaccurate and incomplete results. Using node set however can eliminate such issue, whilst obtaining result which is reliable. Subsequently, both node set and cylinder would be used, depending on the condition.

4.4 Comparative Study between MAT159 and MAT072R3 on Flexural Behaviour Study of RC Beams

4.4.1 B-1Ø12, B-2Ø12, and B-3Ø12 by Almusallam et al. (2015)

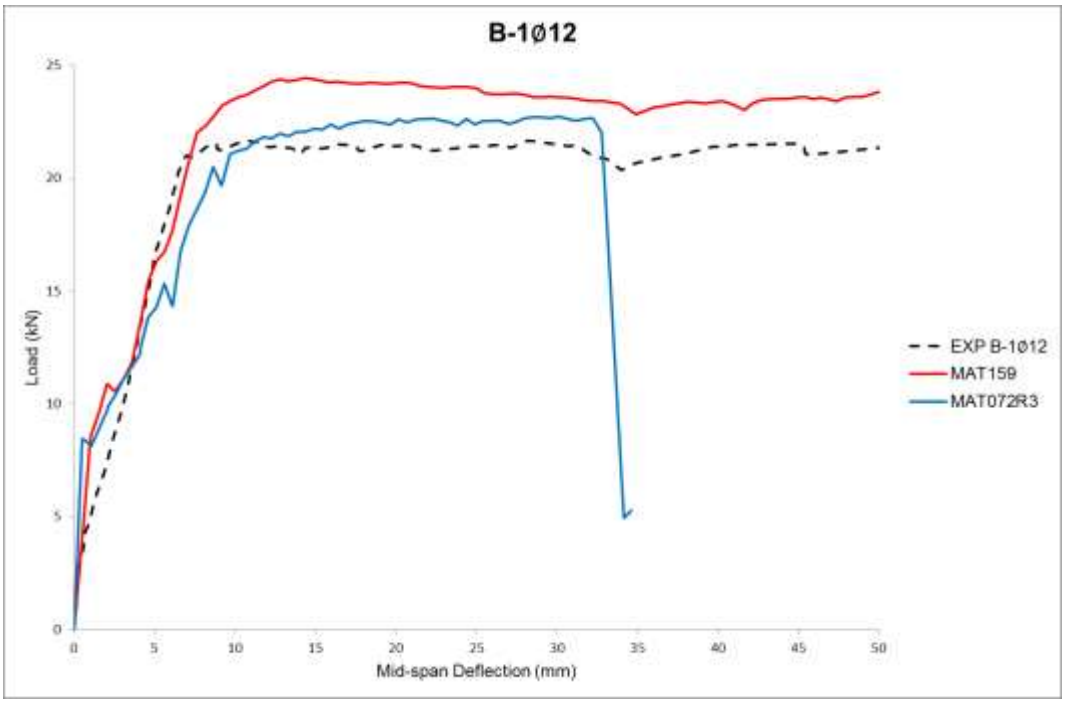

Figure 4.13: Load-deflection curves of beam B-1Ø12 comparing MAT159 and MAT072R3 to experimental results by Almusallam et al. (2015).

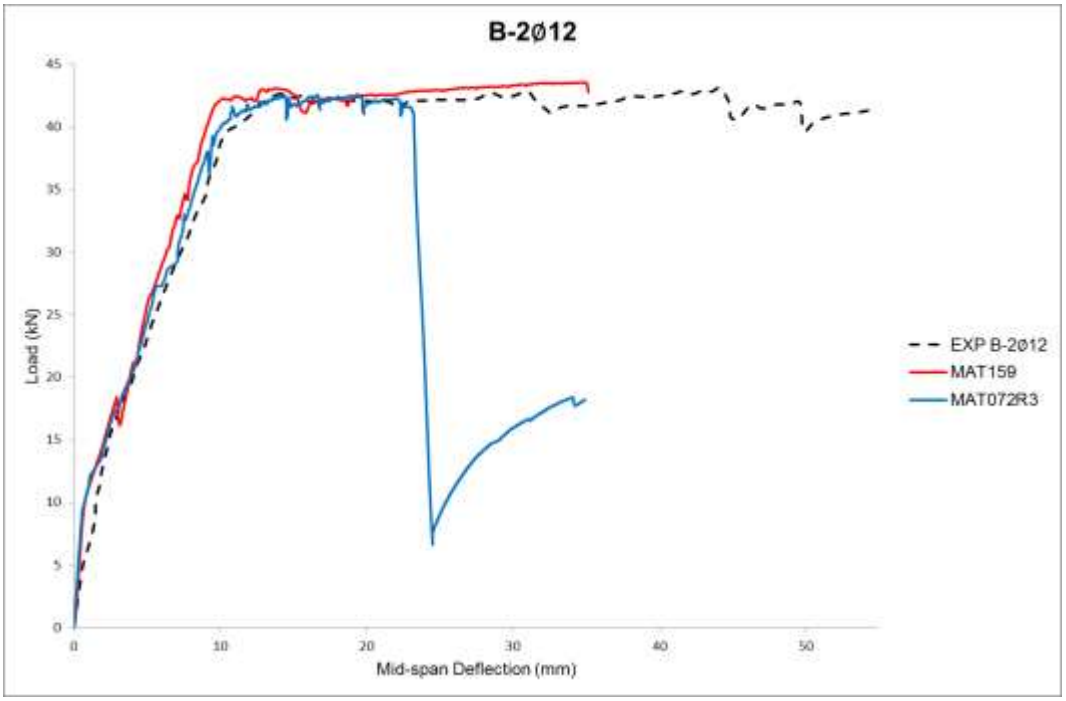

Figure 4.14: Load-deflection curves of beam B-2Ø12 comparing MAT159 and MAT072R3 to experimental results by Almusallam et al. (2015).

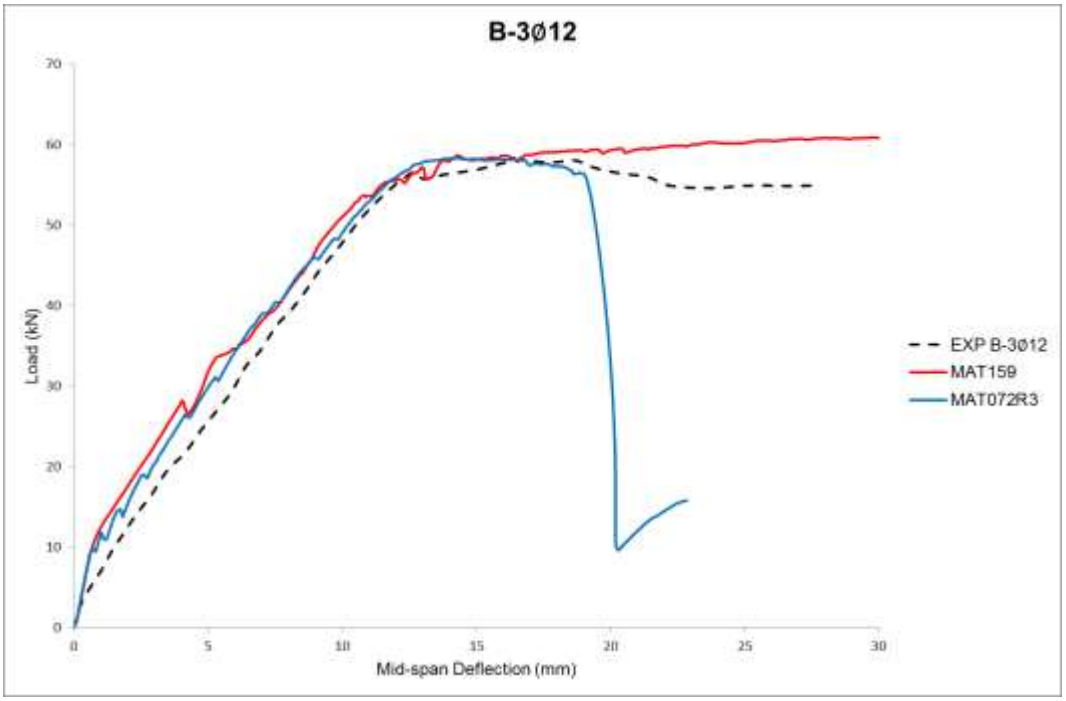

Figure 4.15: Load-deflection curves of beam B-3Ø12 comparing MAT159 and MAT072R3 to experimental results by Almusallam et al. (2015).

From the load-deflection curves shown in Figure 4.13, 4.14, and 4.15, it can be seen that both MAT159 and MAT072R3 correlates well to the experimental load-deflection curves for control beams B-1Ø12, B-2Ø12, and B-3Ø12 respectively, under quasi-static loading rate of 1mm/s. For MAT159, the highest deviation of failure load (from the experimental result) is in the case of B-1Ø12, where the ultimate load deviates at approximately 9.83% from the experimental results, while a deviation of 0.01% and 4.56% are recorded for beam B-2Ø12 and B-3Ø12 respectively. Similarly for MAT072R3, highest deviation of failure load can be seen for B-1Ø12, at 4.64%, and subsequently 3.48% for B-3Ø12 and 1.32% for B-2Ø12.

Referring to the load-deflection curves, it can be seen that MAT159 has exhibited a rather ductile behaviour as compared to MAT072R3. MAT072R3 has shown brittle behaviour. In terms of failure load and stiffness, MAT072R3 correlates well with the experimental results, but not the plastic behaviour at post-yielding stage of the RC beams. Failure modes of control beams B-1Ø12, B-2Ø12, and B-3Ø12 are shown in Figure 4.16, 4.17, and 4.18.

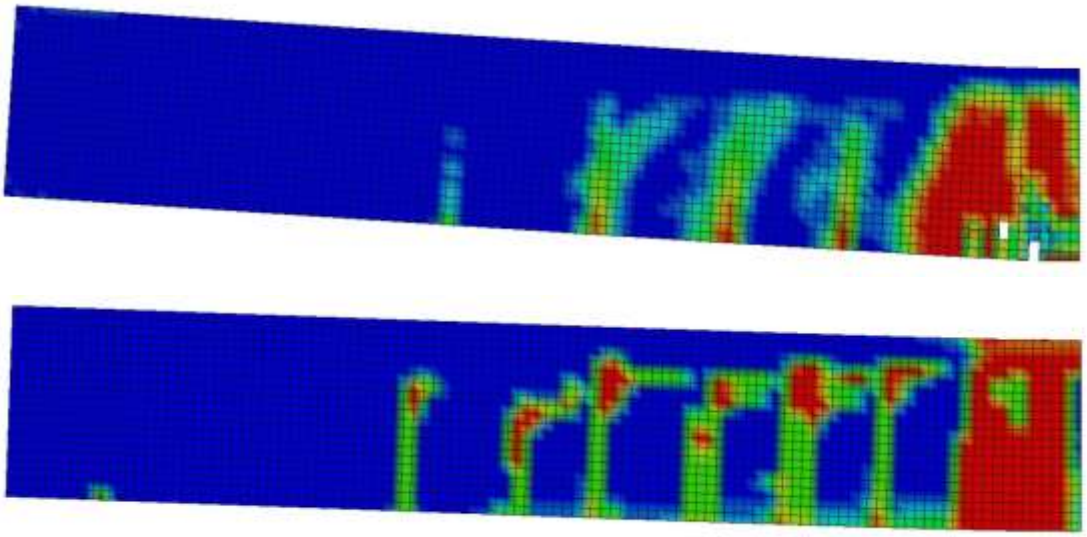

Figure 4.16: Failure mode of B-1Ø12 modelled with MAT159 (above) and MAT072R3 (below).

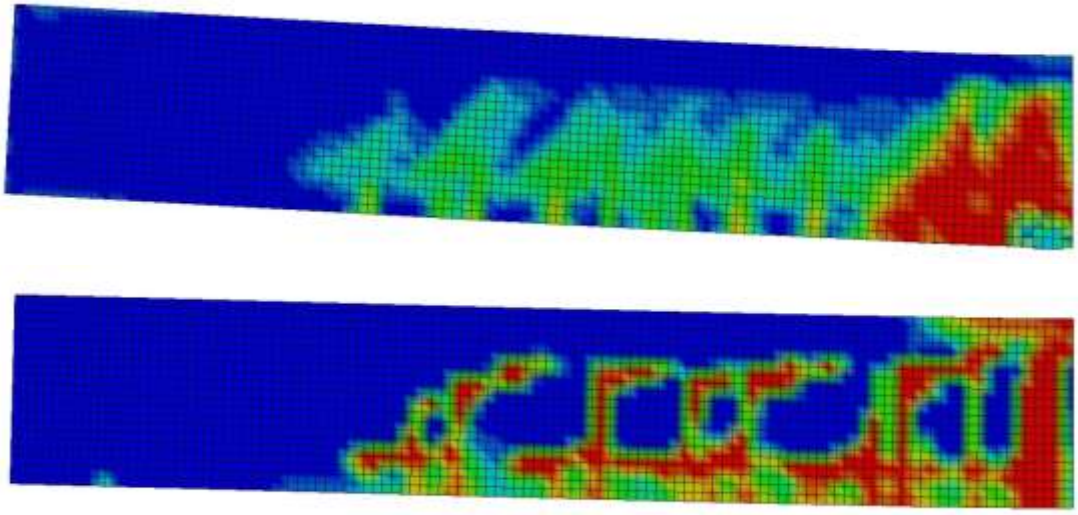

Figure 4.17: Failure mode of B-2Ø12 modelled with MAT159 (above) and MAT072R3 (below).

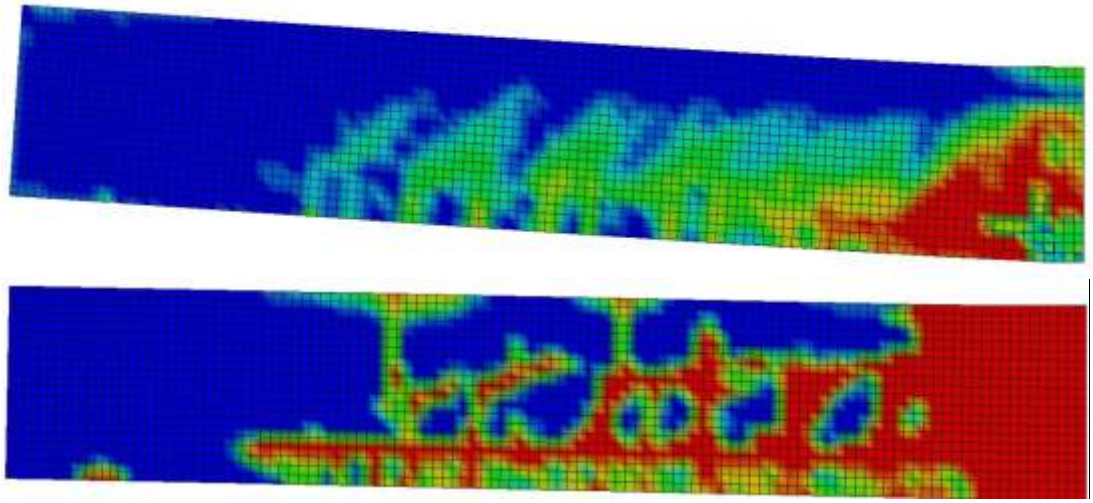

Figure 4.18: Failure mode of B-3Ø12 modelled with MAT159 (above) and MAT072R3 (below).

All failure modes have shown obvious flexural failure at mid-span of all beam models, and then cracks spread to the side towards the support. For MAT159, as erosion option is turned on, at mid-span of the beam it can be seen that concrete crushing occurred causing the elements exceeding the pre-defined plastic strain limit to erode. As in the case of MAT072R3, no such features can be seen, but yet exhibited an obvious flexural failure in mid-span of the beam.

As such, in terms of flexural behaviour, MAT159 and MAT072R3 correlate well to the experimental results in terms of failure load and failure mode. However, in terms of ductility, MAT159 has shown better results as compared to MAT072R3, in which MAT072R3 is rather brittle than MAT159.

4.5 Comparative Study between MAT159 and MAT072R3 on Shear Behaviour Study of RC Beams

4.5.1 B1 Control Beam by Teo & Lau (2015)

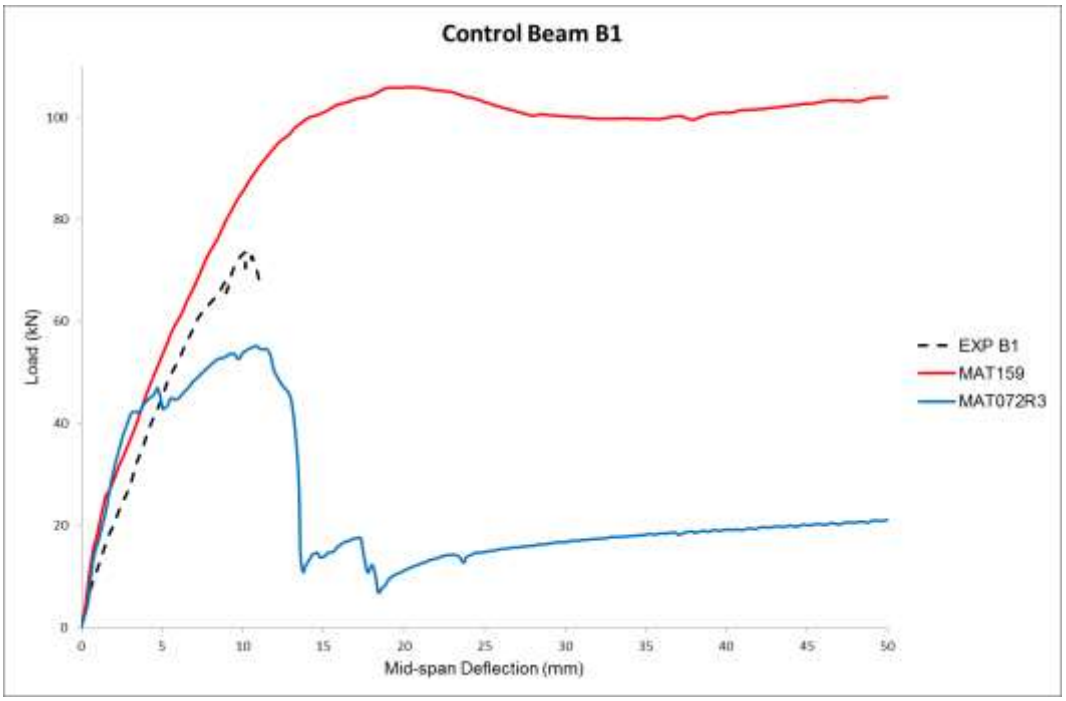

Figure 4.19: Load-deflection curves of control beam B1 comparing MAT159 and MAT072R3 to experimental results by Teo & Lau (2015).

Figure 4.19 shows that neither MAT159 nor MAT072R3 matches well to the experimental results. It is apparent that MAT159 overestimates the stiffness and failure load of the beam while MAT072R3 overestimates the stiffness and underestimates the failure load. Percentage difference for both MAT159 and MAT072R3 in terms of failure load is as high as 33-34%.

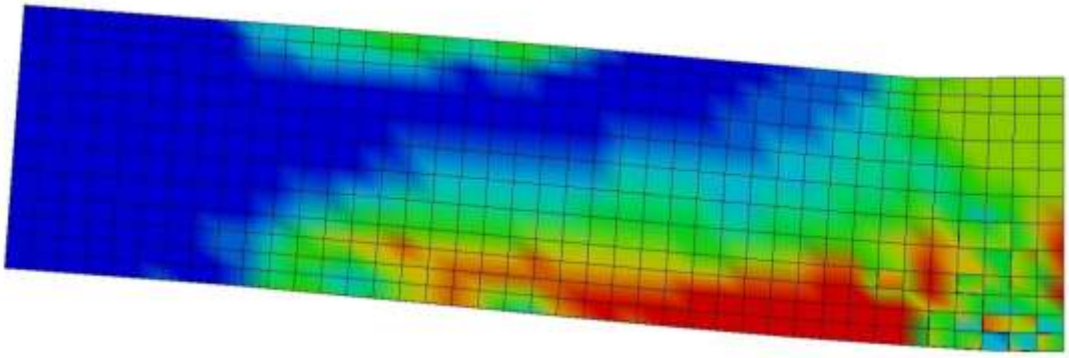

Figure 4.20: Failure mode of control beam B1 modelled with MAT159.

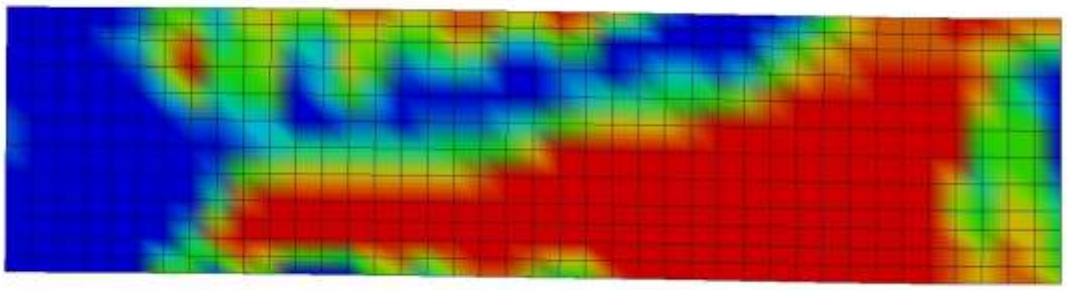

Figure 4.21: Failure mode of control beam B1 modelled with MAT072R3.

In terms of failure mode, MAT072R3 has shown shear behaviour, in which an impression of diagonal shear crack can be seen across the shear span of the beam. As in the case of MAT159, flexural concrete crush can be seen at the mid-span of the beam.

4.5.2 ZC4, ZC6, and ZC6(2) by Zhang & Hsu (2005)

Figure 4.22, 4.23, and 4.24 have shown the load-deflection curves of control beams ZC4, ZC6, and ZC6(2) tested experimentally by Zhang & Hsu (2005). In general, FE results deviate greatly from experimental results in term of load-deflection curve, where a huge difference of stiffness and failure can be seen in numerous cases.

However, generally MAT159 has generated a higher failure load than MAT072R3, in which most are overestimating failure load of the beams.

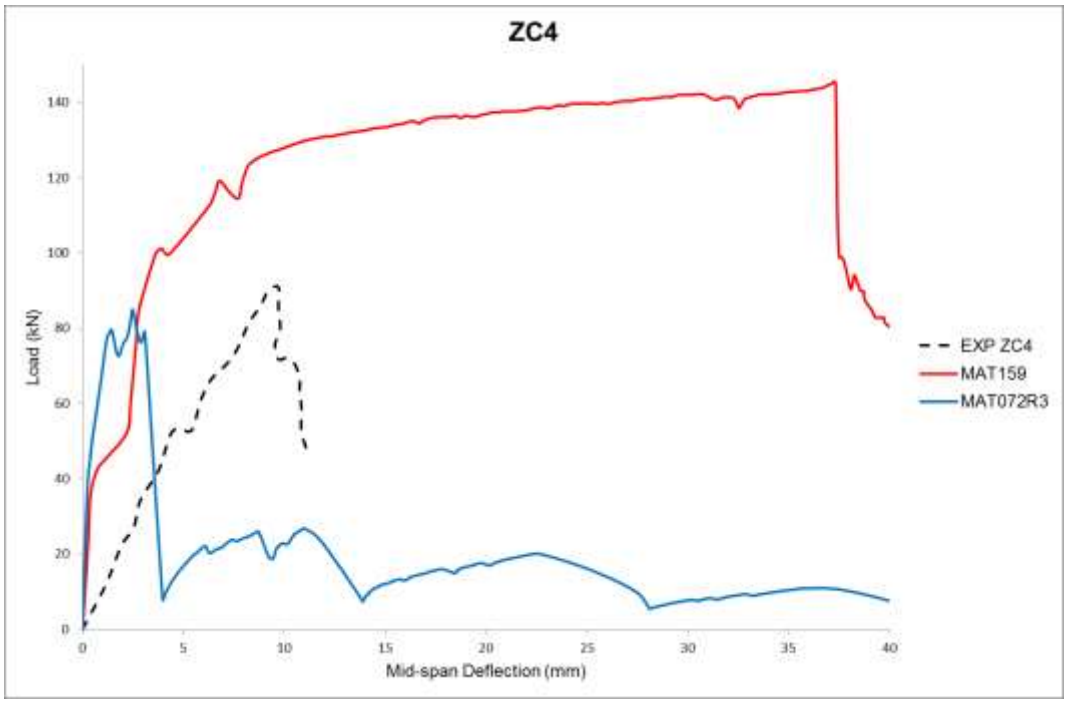

Figure 4.22: Load-deflection curves of control beam ZC4 comparing MAT159 and MAT072R3 to experimental results by Zhang & Hsu (2005).

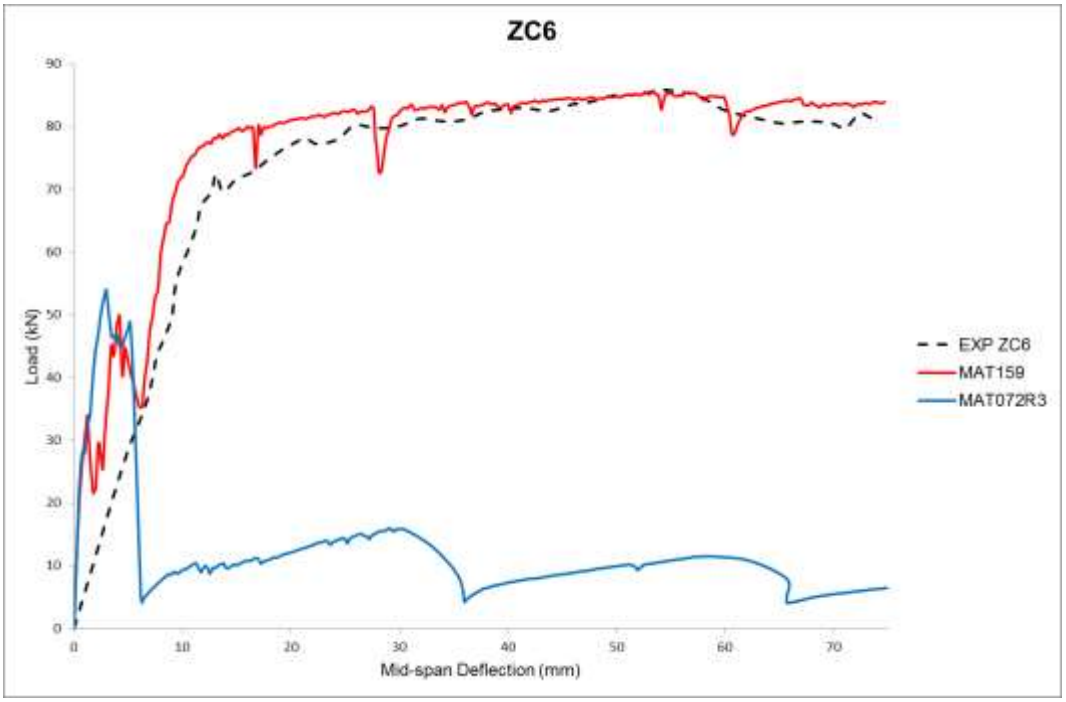

Figure 4.23: Load-deflection curves of control beam ZC6 comparing MAT159 and MAT072R3 to experimental results by Zhang & Hsu (2005).

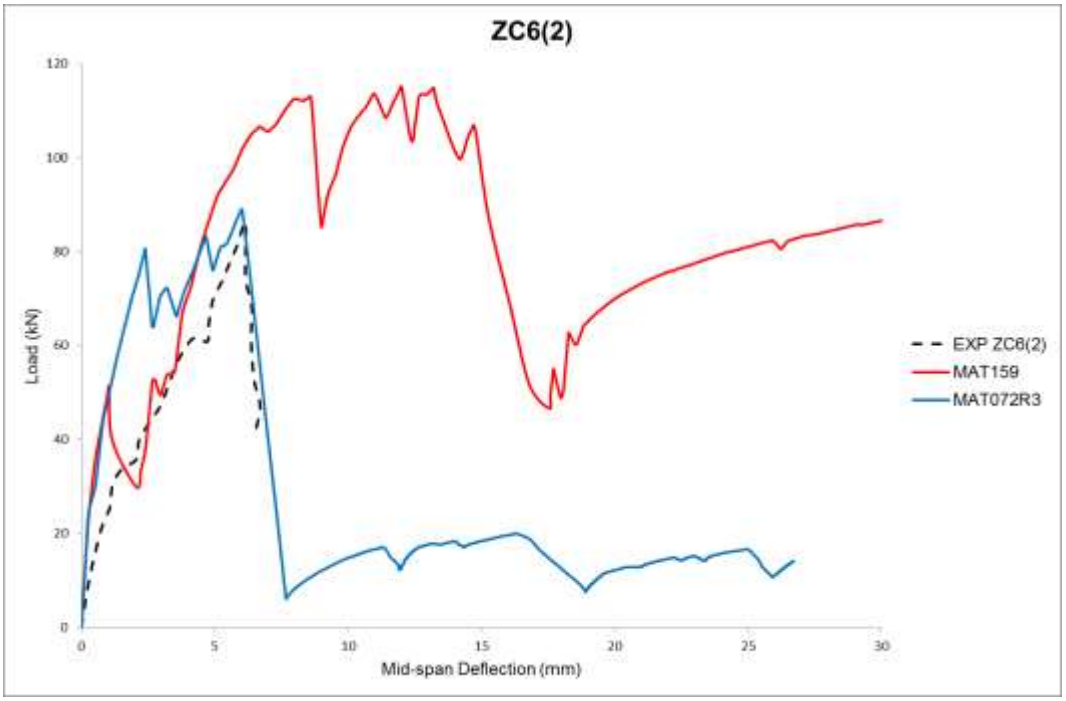

Figure 4.24: Load-deflection curves of control beam ZC6(2) comparing MAT159 and MAT072R3 to experimental results by Zhang & Hsu (2005).

For MAT159, ZC6 has shown rather similar load-deflection curve to the experimental result. FE result has shown an ultimate failure load at 85.67kN, with a percentage difference of 0.17% deviate from the experimental ultimate failure load of 85.82kN. As stated by Zhang & Hsu (2005), the failure mode of ZC6 in the experiment was combined shear and flexure cracking. This might be the reason why MAT159 could predict the ultimate failure load accurately, in which ZC6 is not solely failed in shear.

However, the stiffness of the beam modelled with MAT159 is slightly greater than the experimental results. Pre-yielding behaviour does not exhibit a stable and linear result, which causes MAT159 to be rather unreliable in this sense. Same goes to the other two beams, the ultimate failure load deviates at 36.5% and 25.2% for ZC4 and ZC6(2) respectively. Consequently, MAT159 apparently does not yield reliable results on shear behaviour of RC beams.

As in the case of MAT072R3, FE results of all three control beams have shown that the model is stiffer than experimental result. Despite this, two of the cases have

matched the experimental ultimate load with deviation of 6.99% and 3.24%, which are ZC4 and ZC6(2) respectively. While for ZC6, an ultimate failure load deviation of 58.9% is deduced, significantly lower than that of the experimental result. Most of the beams modelled using MAT072R3 in LS-DYNA are less deformable than the experimental result, in which it reaches failure at a relatively low mid-span deflection. MAT072R3 is thus unreliable in predicting shear behaviour of RC beam loaded under quasi-static loading. Failure modes of beams are shown below.

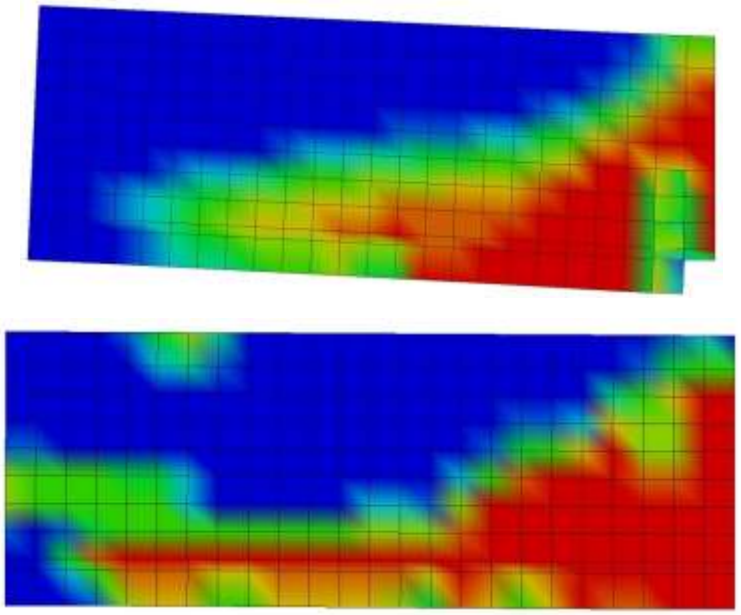

Figure 4.25: Failure mode of ZC4 modelled with MAT159 (above) and MAT072R3 (below).

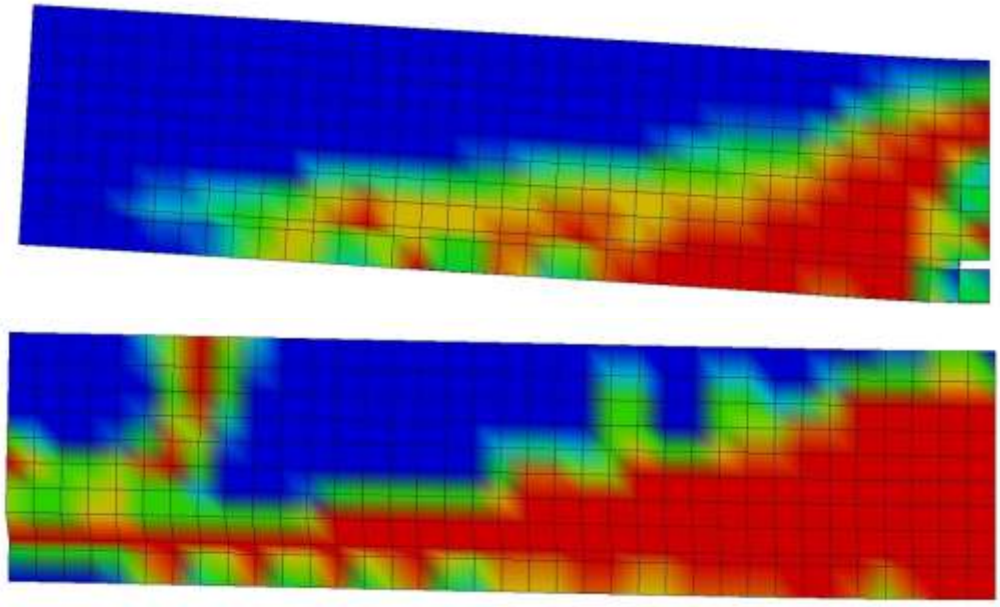

Figure 4.26: Failure mode of ZC6 modelled with MAT159 (above) and MAT072R3 (below).

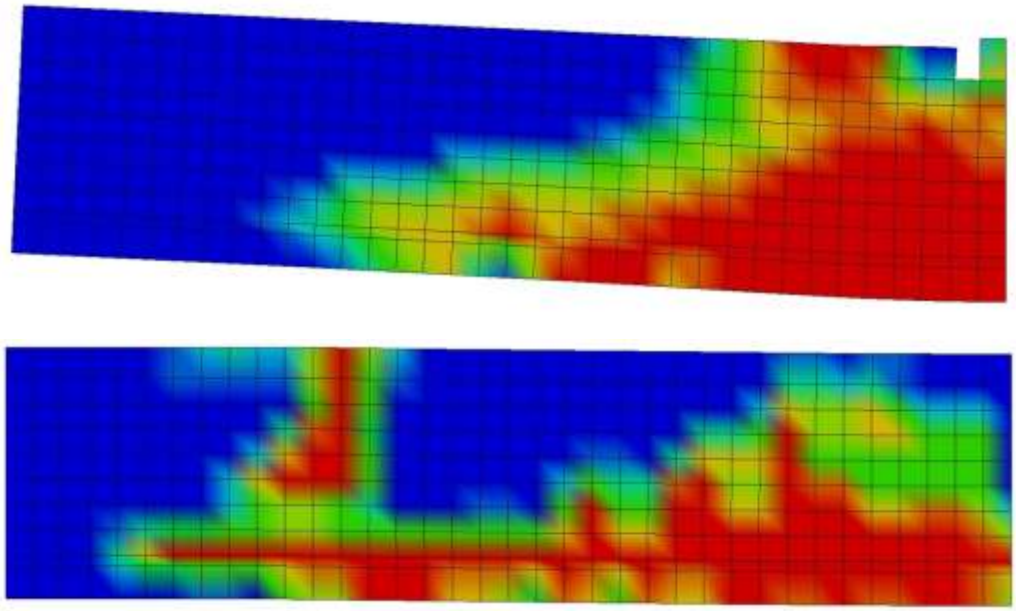

Figure 4.27: Failure mode of ZC6(2) modelled with MAT159 (above) and MAT072R3 (below).

Similarly to control beam B1 by Teo & Lau (2015), MAT072R3 better simulates the failure mode of beams ZC4, ZC6, and ZC6(2). An apparent shear failure can be seen for all three beams. However, for MAT159, concrete crushing can be seen at mid-span of the beam, thus making it seem more like flexural failure or perhaps combination of flexure and shear failure.

Consequently, to sum up comparative study between MAT159 and MAT072R3 on shear behaviour of RC beams under quasi-static loading, generally both concrete materials fail to match experimental results. As there could be numerous factors that influence the FE results, further researches are to be done on modelling shear behaviour of RC beams loaded with quasi-static loading using MAT159 and MAT072R3.

4.6 Calibration of LS-DYNA Model for Concrete Material Model MAT072R3

4.6.1 MAT072R3 – Uniaxial Tensile Strength (FT)

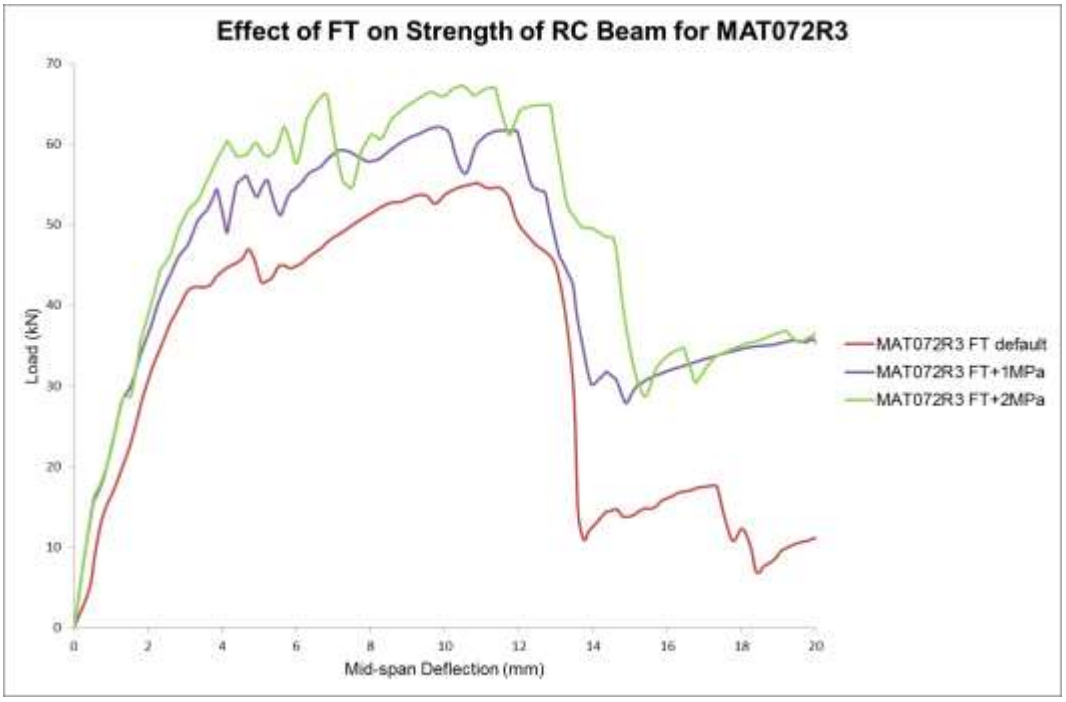

Figure 4.28: Load-deflection curves of RC beam with varying FT.

Figure 4.28 shows the effect of one of the input parameters of MAT072R3, which is uniaxial tensile strength of concrete (FT), on behaviour of RC beams. As shown in Table 4.1, the higher the tensile strength, the higher the ultimate failure loads. This conforms to logic and enables concrete with higher tensile strength to be simulated using MAT072R3.

Table 4.1: FE results of effect of FT on ultimate failure load of RC beam

Test #		Uniaxial Tensile Strength FT (MPa)	Ultimate Failure Load (MPa)
1	Default	2.413	55.17
2	Default + 1MPa	3.413	62.14
3	Default +2MPa	4.413	67.29

4.6.2 MAT072R3 – LOCWIDTH

Figure 4.29 shows the effect of LOCWIDTH (three times the maximum aggregate size) on the load-deflection curves of RC beams loaded under quasi-static loading.

As shown in the load-deflection curves, the greater the maximum aggregate size, the lower the ultimate failure load as well as the mid-span deflection at failure. In terms of stiffness of the beam, LOCWIDTH does not seem to have an effect on it. However, ductility of the beam is dependent on the aggregate size. The greater the aggregate size, the less deformable the beam is with a lower ultimate strain at failure. This has reflect that as the maximum aggregate size increases, interlocking between aggregate is harder to achieve as voids in between aggregates would be relatively larger than specimen with smaller aggregate size. Concrete with higher aggregate sizes is more prone to slip of both aggregate upon loaded with quasi-static loading.

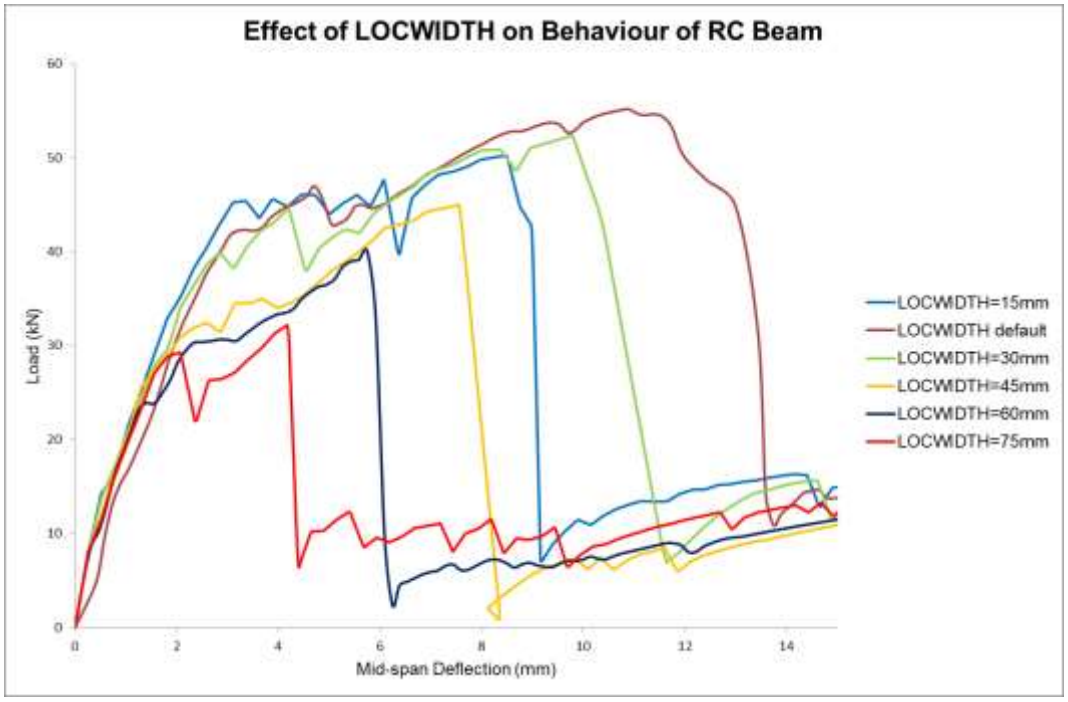

Figure 4.29: Load-deflection curves of RC beam with varying LOCWIDTH.

4.6.3 MAT072R3 – Modulus of Elasticity

As pressure, C2, decreases, the bulk modulus decreases, and eventually modulus of elasticity decreases too. As such, this has been simulated well as shown in Figure 4.30. A decrease in modulus of elasticity of the concrete material itself has caused the modulus elasticity of the whole RC beam decreases as well. In order to determine what input parameter of pressure C2 is to be used, experimental works can be done, or it can be deduced according to good engineering knowledge of material.

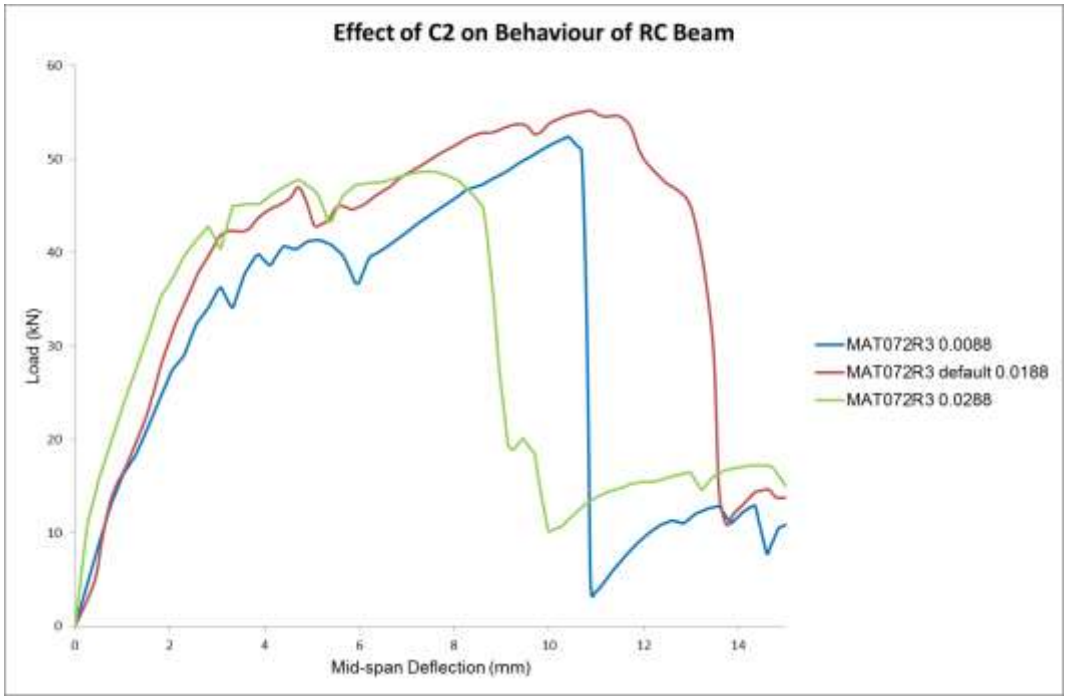

Figure 4.30: Load-deflection curves of RC beam with varying pressure C2.

CHAPTER 5

CONCLUSION & RECOMMENDATION

Despite the fact that LS-DYNA is designed for transient dynamic analysis, it is capable of performing static analysis as well. Quasi-static simulation of RC beams involved displacement-controlled static loading and the loading rate should be low enough to ensure that inertial and damping forces remain negligible. At the same time, the loading rate should not be too slow as it will cost a lot of computational time. An optimum loading rate should be employed to achieve these.

From the single element test, it has provided valuable insights in the effect of several input parameters on the behaviour of concrete material model, including size of element, loading rate, compressive strength, aggregate size, cap retraction option, as well as recovery options. This has also provided the author a better and in-depth view of the material model MAT159. Unfortunately, single element test for MAT072R3 does not work in an appropriate manner. Therefore, the input parameters of MAT072R3, such as uniaxial tensile strength, maximum aggregate size, and modulus of elasticity are studied by using a RC beam specimen.

Half beam modelling has also been validated, thus allowing the simulation works to be carried out more efficiently, since the computational time has been greatly reduced to almost halved. It has also been proven that the FE results have only a minimal effect, regardless of using node set or cylinder for support and load application.

In comparative study between MAT159 and MAT072R3 on flexural behaviour of RC beams, FE results have shown that both material models correlate well to the experimental results, in terms of load-deflection curves. However, MAT072R3 is less ductile than MAT159 and failure modes of MAT159 represent exactly the

experimental failure modes, making MAT159 more applicable for modelling flexural behaviour of RC beams.

As in the case of shear behaviour of RC beams, both material models have shown less promising results. In terms of failure mode, MAT159 have shown behaviour of flexural cracking while MAT072R3 is more conformed to the diagonal shear crack of a beam designed to fail in shear. In terms of failure load, MAT159 often overestimates the ultimate load, while MAT072R3 underestimates the ultimate load in certain cases. However, in terms of stiffness, both material models do not agree to the experimental load-deflection curves and overestimates the stiffness of the beam.

Due to time constraint, mesh convergence test is not carried out for RC beam models used to study shear behaviour of MAT159 and MAT072R3. Further to this research, the RC beams designed to fail in shear shall be modelled using finer mesh and then again verify the reliability of MAT159 and MAT072R3. On top of that, more beam specimens from different researchers should be used to carry out the comparative study between MAT159 and MAT072R3 on concrete behaviour modelling under quasi-static loading, to have a firm and definite conclusion on the reliability of the two material models on quasi-static simulation.

REFERENCES

Abraham, C., & Ong, K. (2015). Performance Of Fibre-reinforced High-strength Concrete With Steel Sandwich Composite Panels Under Static Loading. *WIT Transactions on Modelling and Simulation, 59*, 495-505.

Adhikary, S. D., Li, B., & Fujikake, K. (2012). Dynamic behavior of reinforced concrete beams under varying rates of concentrated loading. *International Journal of Impact Engineering, 47*, 24-38.

Adhikary, S. D., Li, B., & Fujikake, K. (2013). Strength and behavior in shear of reinforced concrete deep beams under dynamic loading conditions. *Nuclear Engineering and Design, 259*, 14-28.

Adhikary, S. D., Li, B., & Fujikake, K. (2015). Low Velocity Impact Response of Reinforced Concrete Beams: Experimental and Numerical Investigation. *International Journal of Protective Structures, 6*(1), 81-112.

Almusallam, T. H., Elsanadedy, H. M., & Al-Salloum, Y. A. (2015). Effect of longitudinal steel ratio on behavior of RC beams strengthened with FRP composites: Experimental and FE study. *Journal of Composites for Construction, 19*(1). doi: 10.1061/(ASCE)CC.1943-5614.0000486

Bhatti, A. Q., Kishi, N., Mikami, H., & Ando, T. (2009). Elasto-plastic impact response analysis of shear-failure-type RC beams with shear rebars. *Materials & Design, 30*(3), 502-510.

Cotsovos, D. M., Zeris, C. A., & Abbas, A. A. (2009). Finite element modeling of structural concrete. *COMPDYN 2009*.

Elsanadedy, H. M., Almusallam, T. H., Alsayed, S. H., & Al-Salloum, Y. A. (2013). Flexural strengthening of RC beams using textile reinforced mortar - Experimental and numerical study. *Composite Structures, 97*, 40-55. doi: 10.1016/j.compstruct.2012.09.053

Hallquist, J. O. (2007). LS-DYNA keyword user's manual. *Livermore Software Technology Corporation, 970*.

Kishi, N., Khasraghy, S. G., & Kon-No, H. (2011). Numerical simulation of reinforced concrete beams under consecutive impact loading. *ACI Structural Journal, 108*(4), 444.

Li, J., & Hao, H. (2011). A two-step numerical method for efficient analysis of structural response to blast load. *International Journal of Protective Structures, 2*(1), 103-126.

Linde, P., Schulz, A., & Rust, W. (2006). Influence of modelling and solution methods on the FE-simulation of the post-buckling behaviour of stiffened aircraft fuselage panels. *Composite Structures, 73*(2), 229-236.

Liu, Y. (2008). ANSYS and LS-DYNA used for structural analysis. *International Journal of Computer Aided Engineering and Technology, 1*(1), 31-44.

LSTC. (2003). LS-DYNA Support: Quasistatic Simulation. Retrieved March 23, 2016, from http://www.dynasupport.com/howtos/general/quasistatic-simulation

LSTC. (2011). LS-DYNA. Retrieved March 23, 2016, from http://www.lstc.com/products/ls-dyna

Magalhaes Pereira, L., Weerheijm, J., & Sluys, L. (2013). *Damage prediction in a concrete bar due to a compression and tension pulse: A comparison of the K&C, the CSCM and the RHT material models in LS-DYNA.* Paper presented at the 15th ISIEMS Conference: International Symposium on the Interaction of the Effects of Munitions with Structures, Potsdam, Germany, 17-20 September 2013; presented paper.

Mohammed, T., & Parvin, A. (2011). *Impact load response of concrete beams strengthened with composites.* Paper presented at the First Middle East Conference on Smart Monitoring, Assessment and Rehabilitation of Civil Structures.

Mosallam, A., Elsanadedy, H. M., Almusallam, T. H., Al-Salloum, Y. A., & Alsayed, S. H. (2015). Structural evaluation of reinforced concrete beams strengthened with innovative bolted/bonded advanced frp composites sandwich panels. *Composite Structures, 124*, 421-440. doi: http://dx.doi.org/10.1016/j.compstruct.2015.01.020

Murray, Y. D. (2007). Users manual for LS-DYNA concrete material model 159.

Murray, Y. D., Abu-Odeh, A. Y., & Bligh, R. P. (2007). Evaluation of LS-DYNA concrete material model 159.

NPTEL, M. I. (Producer). (2014). Dr. R. Krishnakumar: Introduction to Finite Element Method. Retrieved from https://www.youtube.com/watch?v=KR74TQesUoQ

Rajagopal, K. R. (1976). Nonlinear analysis of reinforced concrete beams, beam-columns and slabs by finite elements.

Reddy, J. N. (1993). *An introduction to the finite element method* (Vol. 2): McGraw-Hill New York.

Rust, W., & Schweizerhof, K. (2003). Finite element limit load analysis of thin-walled structures by ANSYS (implicit), LS-DYNA (explicit) and in combination. *Thin-walled structures, 41*(2), 227-244.

Schwer, L. E., & Malvar, L. J. (2005). Simplified concrete modeling with* MAT_CONCRETE_DAMAGE_REL3. *JRI LS-Dyna User Week*, 49-60.

Suidan, M., & Schnobrich, W. C. (1973). Finite element analysis of reinforced concrete. *Journal of the Structural Division, 99*(10), 2109-2122.

Teo, W., & Lau, K. M. H. (2015). *An Experimental Investigation into the Shear Interaction between Internal Stirrups and External FRP Systems of RC Beams*. Paper presented at the IABSE Conference - Structural Engineering: Providing Solutions to Global Challenges, Geneve, Switzerland.

Wu, Y., Crawford, J., Lan, S., & Magallanes, J. (2014). *Validation studies for concrete constitutive models with blast test data.* Paper presented at the Proc., 13th Int. LS-DYNA® Users Conf., LSTC, Livermore, CA.

Yi, Z., Agrawal, A. K., Ettouney, M., & Alampalli, S. (2007). *Finite element simulation of blast loads on reinforced concrete structures using LS-DYNA.* Paper presented at the 2007 Structures Congress: New Horizons and Better Practices.

Yoon, Y. S., Lee, J., Jang, I., & Hwang, D. (2013). *Improved impact resistance of layered steel fiber reinforced concrte beam.* Paper presented at the Hokkaido University collection of Scholarly Academic Papers, HUSCAP.

Zhang, & Hsu, C.-T. T. (2005). Shear strengthening of reinforced concrete beams using carbon-fiber-reinforced polymer laminates. *Journal of Composites for Construction, 9*(2), 158-169.

Zhang, X. H., Wu, Y. Y., & Wang, J. (2011). *Numerical Simulation for Failure Modes of Reinforced Concrete Beams under Blast Loading.* Paper presented at the Advanced Materials Research.